Nucleophilic Addition of Water and Alcohols to Dicyanonitrosomethanide: Ligands with Diverse Bonding Modes in Magnetically Coupled d-Block Complexes

ARTICLE *in* BERICHTE DER DEUTSCHEN CHEMISCHEN GESELLSCHAFT · JANUARY 2010

Impact Factor: 2.94 · DOI: 10.1002/ejic.200900779

6 AUTHORS, INCLUDING:

David R Turner
Monash University (Australia)
104 PUBLICATIONS **2,180** CITATIONS
SEE PROFILE

Boujemaa Moubaraki
Monash University (Australia)
342 PUBLICATIONS **9,400** CITATIONS
SEE PROFILE

Keith S Murray
Monash University (Australia)
552 PUBLICATIONS **14,732** CITATIONS
SEE PROFILE

Stuart R. Batten
Monash University (Australia)
311 PUBLICATIONS **14,406** CITATIONS
SEE PROFILE

DOI: 10.1002/ejic.200900779

Nucleophilic Addition of Water and Alcohols to Dicyanonitrosomethanide: Ligands with Diverse Bonding Modes in Magnetically Coupled d-Block Complexes

Anthony S. R. Chesman,[a] David R. Turner,[a] Boujemaa Moubaraki,[a] Keith S. Murray,[a] Glen B. Deacon,[a] and Stuart R. Batten*[a]

Keywords: Self-assembly / Magnetic properties / Transition metals / Coordination modes / In situ synthesis

Ligands resulting from the transition-metal-promoted nucleophilic addition of water or an alcohol to dicyanonitrosomethanide ions (dcnm) have been utilised in the formation of a large series of polynuclear complexes. Addition of water to dcnm results in formation of carbamoylcyanonitrosomethanide (ccnm); deprotonation of this ligand gives amidocarbonyl(cyano)nitrosomethanide (acnm), which has been incorporated into the trinuclear complex $[Cu_3(acnm)_2(dmae)_2(H_2O)_2]$ [dmae = 2-(dimethylamino)ethoxide] (**1**) which shows strong antiferromagnetic coupling with an exchange coupling constant, $J = -500\ cm^{-1}$. $[Cu(acnm)(NH_3)_2]_\infty$ (**2**) marks the first instance of acnm facilitating the formation of a coordination polymer, namely a 1D chain with intramolecular hydrogen bonding. Attempts to synthesise **2** through different reaction conditions instead resulted in the mononuclear $[Cu(acnm)(NH_3)_2(py)]$ (py = pyridine) (**3**). The addition of ethanol to dcnm results in cyano[imino(ethoxy)methyl]nitrosomethanide (cenm) which features in the mononuclear $[Cu(cenm)_2(H_2O)_2]$ (**4**) and polymeric $\{[Cu(cenm)_2]_2{\cdot}H_2O\}_\infty$ (**5**). The latter is the first example of the cenm ligand in a coordination polymer and has a highly unusual coordination mode through the nitrile groups and extremely weak antiferromagnetic coupling. $\{[Mn_3(ccnm)_2(EtOH)_2(OAc)_4]{\cdot}2EtOH\}_\infty$ (**6**) and $(Et_4N)_2[Cu(ccnm)_4]$ (**7**) contain previously unobserved coordination modes of the ccnm ligand while the complex $[Mn(cmnm)_3Mn(bipy)(MeOH)](ClO_4)$ (**8**) {cmnm = cyano[imino(methoxy)methyl]nitrosomethanide, bipy = 2,2′-bipyridine} displays weak antiferromagnetic coupling between manganese atoms with $J = -1.44\ cm^{-1}$. A change in the solvent systems used in the synthesis of **7** results in the formation of the mononuclear complexes $[Mn(bipy)_2(dcnm)_2]$ (**9**) or $[Mn(bipy)_2(H_2O)(dcnm)](dcnm){\cdot}H_2O$ (**10**) and $[Mn(bipy)_2(dcnm)(H_2O)](dcnm)$ (**11**). The addition of ethlyene glycol monomethyl ether to dcnm gives cyano[imino(2-methoxyethoxy)methyl]nitrosomethanide (cgnm) and the formation of $[Cu(cgnm)_2(H_2O)_2]$ (**12**).

Introduction

Pseudohalide ligands such as cyanate,[1] dicyanamide,[2,3] tricyanomethanide[4] and carbamoyldicyanomethanide[5] display a propensity to undergo transition-metal-promoted nucleophilic addition. This reaction is also observed with dicyanonitrosomethanide, $C(CN)_2(NO)^-$ (dcnm), where the addition of water or methanol to a nitrile group results in the formation of carbamoylcyanonitrosomethanide (ccnm) and cyano[imino(methoxy)methyl]nitrosomethanide (cmnm) ions, respectively (Scheme 1).[6] Recently the library of dcnm derivatives has been extended by using amines such as 1,2-diaminoethane as nucleophiles, which may add to both nitrile arms and cyclise to form diimidazolinylnitrosomethanide (dinm).[7] The use of acids may also promote nulceophilic addition but the resulting protonation of the nitroso group to give an oxime results in neutral products with more limited available coordination modes.[8]

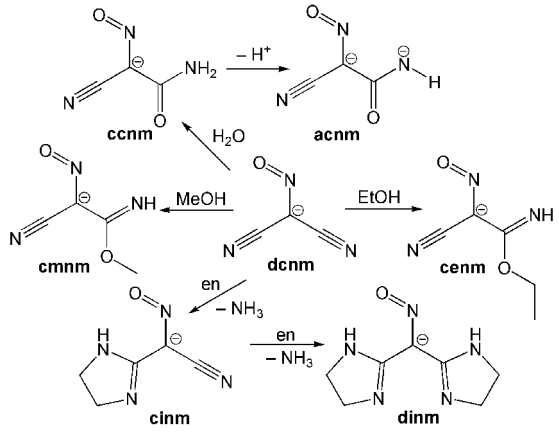

Scheme 1. Products resulting from nucleophilic addition of alcohols and amines to dcnm.

Despite the apparent divergent nature of these nitroso/cyano ligands they generally form mononuclear complexes and their role in the formation of clusters or coordination polymers is yet to be fully realised. Exceptions to this are salts of dcnm[9,10] and dicyanonitromethanide,[11] $C(CN)_2$-

[a] School of Chemistry, Monash University,
Wellington Rd, Clayton, Victoria 3800, Australia
Fax: +61-3-99054597
E-mail: stuart.batten@sci.monash.edu.au

$(NO_2)^-$, which crystallise as coordination polymers, and a limited number of polynuclear complexes containing addition derivative ligands.[12–16]

More recently ccnm has been included in "lanthaballs", large polycarbonatolanthanoid clusters in which the ligands act as η^2-nitroso-bound capping species.[17] The related ligand carbamoyldicyanomethanide, known for its participation in numerous hydrogen bond motifs,[18–22] has undergone a similar nucleophilic addition of methanol in the formation of a novel network of Fe^{III}_{10} clusters.[23] Because the pseudohalide ligands dicyanamide, $N(CN)_2^-$, and tricyanomethanide, $C(CN)_3^-$, demonstrate versatility in the formation of coordination polymers, which have garnered much attention for their magnetic properties,[24] and because the solvothermally synthesised $[Cu(cmnm)_2]_\infty$ network demonstrates ferromagnetic coupling,[25] there is a strong impetus to incorporate dcnm-derived ligands in coordination polymers. Related cyanoxime-based complexes have been noted for their cytotoxicity, with their continued development for anti-cancer applications of interest to researchers.[26]

While we have reported a metal-free synthesis of the ccnm anion[17] the formation of other nucleophilic addition products still relies on the presence of a transition metal. In situ formation has proven to be a reliable and repeatable synthetic approach with this class of ligands and gives access to more exotic ligand derivatives. A reaction of ccnm with a base results in subsequent deprotonation to form the unusual dianionic amidocarbonyl(cyano)nitrosomethanide (acnm) ligand. It has previously been reported only in the complexes $(Me_4N)_2[Ni(acnm)_2]\cdot 2H_2O$ and $[(Ph_4Sb)_2Ni(acnm)_2]$ but was formed from an alternate synthesis, namely the double deprotonation of 2-cyano-2-(hydroxyimino)acetamide by hydroxide.[27]

The only evidence of larger alcohols reacting with dcnm is the report of addition of ethanol to form cyano[imino(ethoxy)methyl]nitrosomethanide (cenm).[28] This preliminary account hints at the possibility of further derivatisation of the dcnm ligand by alcohols to add targeted functionality.

The first component of this paper details the nucleophilic addition of water or alcohols to dcnm under varying reaction conditions, examining the effects of differing bases, co-ligands and solvent mixtures on the resulting products. The following section shows how these ligands demonstrate a diverse range of coordination modes in their structures, with their incorporation into series of mono- or polynuclear metal complexes and coordination polymers. The magnetic properties of selected complexes are also discussed.

Results and Discussion

Synthesis

Details of reactions of dcnm with water or an alcohol in the presence of a transition-metal ion and various co-ligands, together with the resulting products, are shown in Table 1. The transition-metal-promoted nucleophilic addition of water to a nitrile group of dcnm results in the formation of carbamoylcyanonitrosomethanide (ccnm) which may then undergo deprotonation of the carbamoyl group to form amidocarbonyl(cyano)nitrosomethanide (acnm) ions (Scheme 1). Thus the reaction of Na(dcnm), copper perchlorate and 2-(dimethylamino)ethanol (dmaeH) in water results in the formation of blue tabular crystals of the product $[Cu_3(acnm)_2(dmae)_2(H_2O)_2]$ [dmae = 2-(dimethylamino)ethoxide] (**1**) in high yield. In the formation of **1**, the excess of dmeaH acts as a base to deprotonate both ccnm and other dmeaH molecules to form the acnm and dmae ions incorporated into **1**. The use of the tertiary amine obviates nucleophilic addition which has been shown to occur preferentially with primary amines in comparison to the addition of alcohols.[7]

The acnm ligand also features in the coordination polymer $[Cu(acnm)(NH_3)_2]_\infty$ (**2**) which forms a blue crystalline product from reaction of (Me_4N)(dcnm), copper perchlorate and aqueous ammonia in a water/pyridine solution. The excess of ammonia deprotonates ccnm to form acnm in this case. Attempts to repeat the synthesis of complex **2**

Table 1. Reactions of $Na/Me_4N/Et_4N$ dcnm salts with transition-metal salts, nucleophilic solvents and co-ligands.

Ligand salt	Metal reagent	Solvent and/or nucleophile[a]	Co-ligand	Product[b]	
Na(dcnm)	$Cu(ClO_4)_2\cdot 6H_2O$	H_2O[a]	dmae	$[Cu_3(\textit{acnm})_2(dmae)_2(H_2O)_2]$[c]	**1**
(Me_4N)(dcnm)	$Cu(ClO_4)_2\cdot 6H_2O$	py/H_2O[a]	NH_3	$[Cu(\textit{acnm})(NH_3)_2]_\infty$[c]	**2**
(Et_4N)(ccnm)	$Cu(ClO_4)_2\cdot 6H_2O$	py/H_2O[a]	NH_3	$[Cu(\textit{acnm})(NH_3)_2(py)]$[c]	**3**
(Me_4N)(dcnm)	$Cu(NO_3)_2\cdot 3H_2O$	EtOH[a]	–	$\{[Cu(\textit{cenm})_2]_2\cdot H_2O\}_\infty$	**4**
Na(dcnm)	$Cu(NO3)_2\cdot 3H_2O$, $Gd(NO_3)_3\cdot 6H_2O$	EtOH[a]	–	$[Cu(\textit{cenm})_2(H_2O)_2]$	**5**
Na(dcnm)	$Mn(OAc)_2\cdot 4H_2O$	EtOH/H_2O[a]	–	$\{[Mn_3(\textit{ccnm})_2EtOH_2(OAc)_4]\cdot 2EtOH\}_\infty$	**6**
(Et_4N)(ccnm)	$CuCl_2\cdot 2H_2O$, $LaCl_3\cdot 7H_2O$	MeOH	–	$(Et_4N)_2[Cu(ccnm)_4]$	**7**
Na(dcnm)	$Mn(ClO_4)_2\cdot 6H_2O$	MeOH[a]	2,2′-Bipy	$[Mn(\textit{cmnm})_3Mn(bipy)(MeOH)](ClO_4)$	**8**
(Me_4N)(dcnm)	$Mn(ClO_4)_2\cdot 6H_2O$	MeOH/H_2O	2,2′-Bipy	$[Mn(bipy)_2(dcnm)_2]$	**9**
(Me_4N)(dcnm)	$Mn(ClO_4)_2\cdot 6H_2O$	MeOH/H_2O	2,2′-Bipy	$[Mn(bipy)_2(dcnm)(H_2O)](dcnm)$	**10**
(Me_4N)(dcnm)	$Mn(ClO_4)_2\cdot 6H_2O$	MeOH/H_2O	2,2′-Bipy	$[Mn(bipy)_2(dcnm)(H_2O)](dcnm)\cdot H_2O$	**11**
(Me_4N)(dcnm)	$Cu(ClO_4)_2\cdot 6H_2O$	2-methoxyethanol[a]	–	$[Cu(\textit{cgnm})_2(H_2O)_2]$	**12**

[a] Solvent that has acted as nucleophile. [b] Ligands resulting from nucleophilic addition are italicised. [c] Ligand from deprotonation of ccnm.

from (Et_4N)(ccnm) rather than (Me_4N)(dcnm) resulted in the discrete mononuclear complex $[Cu(acnm)(NH_3)_2(py)]$ (**3**). The formation of a different product may be due to the presence of a different counter-cation or through an alteration of the self assembly process as the preformed ccnm ligand is used as a reactant.

The only prior report of the transition-metal-promoted nucleophilic addition of ethanol to a nitrile group of dcnm to form cyano[imino(ethoxy)methyl]nitrosomethanide (cenm), is a brief mention of the synthesis and structure of $[Cu(cenm)_2(H_2O)_2]$ (**4**).[28] The synthetic and crystallographic details, however, are unavailable in this report. In our studies we found that crystals of mononuclear **4** began to form from an ethanolic reaction solution containing copper nitrate and (Me_4N)(dcnm) after one month.

In contrast the presence of gadolinium nitrate in an ethanolic reaction solution containing Na(dcnm) and copper nitrate resulted in the formation of the 2D sheet coordination polymer $\{[Cu(cenm)_2]_2 \cdot H_2O\}_\infty$ (**5**), although the lanthanoid metal does not feature in the structure. Without gadolinium nitrate present only crystallisation of **4** is observed. This phenomena of gadolinium influencing the self-assembly of a complex, possibly through pre-coordination of the ligand, without appearing in the final complex has been observed previously.[29]

Throughout our studies of ligands forming from the derivatisation of dcnm we have not previously observed formation of the cenm ligand (Scheme 1), despite repeated uses of ethanol as a solvent for crystallisation. It may be that the ethyl substituent has a solubilising effect on the ligand, limiting the ability of complexes containing the ligand to crystallise from solution. Alternatively, the relative rarity of the in situ formation of cenm may be indicative of the effect of the steric bulk of the nucleophile in reducing the rate of reaction. The argument for a lowered reactivity with ethanol is further supported by the formation of $\{[Mn^{II}_3(ccnm)_2(EtOH)_2(OAc)_4] \cdot 2EtOH\}_\infty$ (**6**), which is synthesised by a reaction of Na(dcnm) and manganese(II) acetate in a water/ethanol (1:4) solution. The excess of ethanol is insufficient to yield the ethanol addition product with the water addition product, ccnm, being favoured.

Complex **7**, $(Et_4N)_2[Cu(ccnm)_4]$, was synthesised by the reaction of preformed ccnm, in the form of the tetraethylammonium salt, and copper chloride in methanol in the presence of lanthanum chloride. A similar reaction solution without lanthanum chloride failed to yield any crystals, again indicating that the lanthanoid plays a role templating product formation.

Reaction of Na(dcnm) and manganese perchlorate with the co-ligand 2,2′-bipyridine in methanol leads to the nucleophilic addition of methanol with the formation of cyano[imino(methoxy)methyl]nitrosomethanide (cmnm) in the complex $[Mn(cmnm)_3Mn(bipy)(MeOH)](ClO_4)$ (**8**). When this complex is viewed in conjunction with the formation of $[Mn^{II}_2Mn^{III}(cmnm)_6](NO_3)$,[12] which also contains the $[Mn^{II}(cmnm)_3]$ moiety and was not synthesised in the presence of 2,2′-bipyridine, it would suggest that the co-ligand caps one face of the other manganese atom, stopping the assembly of the trinuclear complex. The crystal structure of **8**·3.4MeOH contains methanol disordered within the lattice but upon isolation of the bulk product the lattice methanol molecules are exchanged for atmospheric moisture (see Exp. Sect.).

The solvent used in the synthesis of **8** plays a major role in the product isolated. A synthesis using only methanol results in complex **8** while the use of a mixed water/methanol solvent system gives a mononuclear complex where unreacted dcnm coordinates to the manganese atom through the oxygen atom of the nitroso group in $[Mn(bipy)_2(dcnm)_2]$ (**9**). The use of a purely aqueous reaction solution results in complexes with dcnm as a free anion which participates in hydrogen bonding in the lattice, seen in $[Mn(bipy)_2(dcnm)(H_2O)](dcnm) \cdot H_2O$ (**10**) and $[Mn(bipy)_2(dcnm)(H_2O)](dcnm)$ (**11**). Although this is an unusual result when water is used as a solvent and where ccnm formation can be expected, dcnm has been previously been included into transition-metal complex crystal structures without undergoing nucleophilic addition of the protic solvent.[30,31] This may be due to the 2,2′-biypridine in the coordination sphere of the metal centre limiting its ability to promote the nucleophilic addition to the anion.

A reaction of (Me_4N)(dcnm) and copper perchlorate in ethylene glycol monomethyl ether results in the addition of the protic solvent to form cyano[imino(2-methoxyethoxy)methyl]nitrosomethanide (cgnm) observed in the discrete complex $[Cu(cgnm)_2(H_2O)_2]$ (**12**) (Scheme 2). The addition of ethylene glycol monomethyl ether to dcnm involves the largest known nucleophile yet added to the dcnm molecule through this reaction route. This product could not be isolated by crystallisation from the reaction solution, but required the complete evaporation of the solvent to yield green tabular crystals. As observed in the formation of cenm, this may be the result of the dangling methoxyethyl group increasing the solubility of the product and prohibiting facile crystallisation.

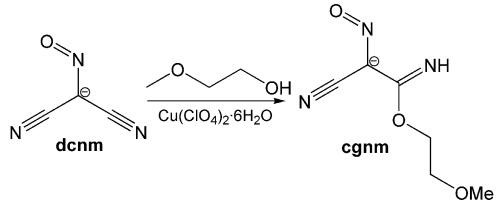

Scheme 2. Addition of ethylene glycol monomethyl ether to dcnm to form cgnm.

Crystal Structures and Magnetism

Complex $[Cu_3(acnm)_2(dmae)_2(H_2O)_2]$ (**1**) crystallises from water in the space group $P\bar{1}$, with half of the molecule contained within the asymmetric unit. The complex contains two square-pyramidal copper atoms flanking a central square-planar copper atom which lies on an inversion center (Figure 1, a). The coordination spheres of the outer copper atoms contain equatorially chelating acnm and dmea

ligands, and a water molecule in one axial position. This axial coordination is Jahn–Teller distorted with a bond length of 2.308(4) Å, longer than that of the oxygen atom of the dmae ligand that coordinates in an basal position with a bond length of 1.909(4) Å The outer copper atoms are bridged to the central copper atom through the nitroso groups of the acnm ligand and the oxygen atom of dmae ligand, resulting in μ_2-η^2(N,N′)Cu:η^1(O)Cu′ and μ_2-η^2(N,O)Cu:η^1(O)Cu′ coordination modes of the respective ligands (Table 2).

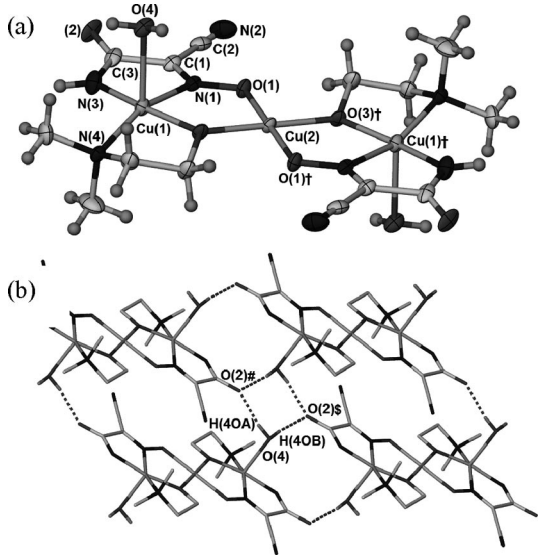

Figure 1. (a) Crystal structure of $[Cu_3(acnm)_2(dmae)_2(H_2O)_2]$ (**1**). Ellipsoids shown at 50% probability. (b) Hydrogen bonding in the crystal structure of **1**. Hydrogen atoms not participating in hydrogen bonding are omitted for clarity. Key hydrogen bond lengths [Å] and angles [°]: O(4)···O(2)$^{\#}$ 2.729(6); O(4)–H(4OA)···O(2)$^{\#}$ 164; O(4)···O(2)$^{\$}$ 2.760(6); O(4)–H(4OB)···O(2)$^{\$}$ 168. Symmetry elements used: † –*x*, –*y*, –*z*; $^{\#}$ *x* – 1, *y*, *z*; $^{\$}$ 1 – *x*, –*y*, –*z* – 1. Hydrogen atoms were refined in restrained positions.

Table 2. Selected bond lengths [Å] and angles [°] of complex **1**.[a]

Cu(1)···Cu(2)	3.3080(7)	Cu(1)···Cu(1)†	6.6160(14)
Cu(1)–N(1)	1.984(5)	N(1)–Cu(1)–N(3)	81.9(2)
Cu(1)–N(3)	1.930(6)	N(4)–Cu(1)–O(3)	86.6(2)
Cu(1)–N(4)	2.020(5)	Cu(1)–O(3)–Cu(2)	120.6(2)
Cu(1)–O(3)	1.909(4)	Cu(1)–N(1)–O(1)	124.5(4)
Cu(1)–O(4)	2.308(4)	N(1)–O(1)–Cu(2)	121.4(5)
Cu(2)–O(1)	1.971(4)	O(1)–Cu(2)–O(3)	91.3(2)
Cu(2)–O(3)	1.900(4)	N(1)–Cu(1)–O(4)	92.5(2)
N(1)–O(1)	1.314(6)	N(4)–Cu(1)–O(4)	105.8(2)
C(1)–N(1)	1.288(8)	O(1)–N(1)–C(1)	121.4(5)
N(3)–C(3)	1.323(9)	N(3)–C(3)–O(2)	129.9(6)
O(2)–C(3)	1.246(8)		

[a] Symmetry element used: † –*x*, –*y*, –*z*.

Crystal packing shows that 2D sheets form as each water molecule hydrogen bonds to the oxygen atoms of the amide groups belonging to two adjacent complexes. The oxygen atoms act as bifurcated hydrogen-bond acceptors (Figure 1, b). Interestingly, the nitrile groups do not participate in any hydrogen bonding and are directed into the spaces between the 2D sheets. There are no significant interactions between sheets.

The magnetic properties of **1** are interesting because they allow us to probe the magnetic exchange coupling across the doubly bridged nitroso/alkoxo combination in the linear Cu^{II}_3 moieties. A plot of effective magnetic moment, per Cu_3, shown in part a of Figure 2, reveals that the μ_{eff} values remain constant, at $\chi_M T$ = 0.405 cm^3 mol^{-1} K (1.8 μ_B), over the 300 to 4 K range with a small decrease then occurring to reach 0.38 cm^3 mol^{-1} K (1.76 μ_B) at 2 K. The corresponding molar susceptibility data, χ_M, is close to Curie-like in its temperature dependence (C = 0.4 cm^3 mol^{-1} K; θ = –0.4 K). This behaviour is characteristic of an isolated S = 1/2 state being thermally populated, this ground state arising through strong antiferromagnetic coupling between the terminal and central Cu atoms across the double bridges. Alkoxo (oxygen sp^2) bridging and oximato [Cu–N(R)O–Cu] bridging are known[32,33] to provide very effective superexchange pathways, augmented in **1** by the close-to-coplanar equatorial planes of the three Cu centres. Thus the efficient overlap of the Cu($d_{x^2-y^2}$) "magnetic orbitals" leads to strong, net antiferromagnetic coupling. A good fit was obtained using a S = 1/2 trimer model[34] using the parameters g = 2.08, $2J$ = –1000 cm^{-1}, Na = 65 × 10^{-6} cm^3 mol^{-1}. Other trinuclear Cu^{II} compounds reported to show such behaviour include the linear $[Cu_3\{C_2S_2(NCH_2CH_2CH_2SCH_2CH_2OH)_2\}_2](ClO_4)_2$[34] and the non-linear $[Cu_3(Me_3tacn)_2(dmg)_2Br](ClO_4)$·MeOH ($Me_3$-tacn = 1,4,7-trimethyl-1,4,7-triazacyclononane; dmg = dimethylglyoximate),[35] the latter having similar Cu–NO–Cu pathways to those in **1**.

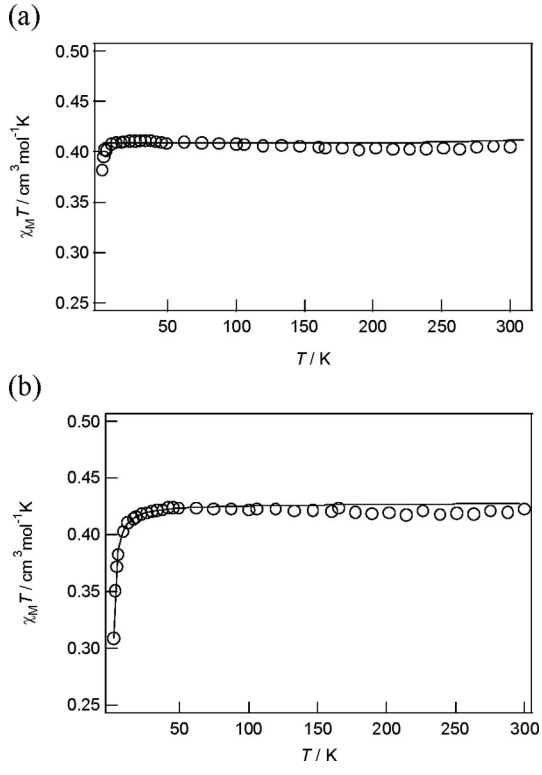

Figure 2. (a) Plot of $\chi_M T$, per Cu_3, for complex **1**. (b) Plot of $\chi_M T$, per Cu, for complex **5**. The solid lines are the calculated plots using the parameters given in the text.

Complex $[Cu(acnm)(NH_3)_2]_\infty$ (**2**) crystallises in the space group $P2_1/n$ with a single moiety of the repeating unit within the asymmetric unit. The basal positions of each square-pyramidal copper atom are occupied by two *cis* ammonia molecules and one acnm ligand chelating in a similar fashion to those in complex **1**. The coordination sphere is completed by the oxygen atom of a nitroso group from another acnm ligand of an adjacent $[Cu(acnm)(NH_3)_2]$ moiety, facilitating the formation of 1D chains (Figure 3, a). As with complex **1**, the acnm ligand has a μ_2-η^2(N,N′)-Cu:η^1(O)Cu′ coordination mode but now with a Jahn–Teller distorted axial bonding mode to a neighbouring copper atom rather than the in plane bridging observed in **1**. The perpendicular bridging mode has previously been reported for this class of ligands only in the $[Cu(cmnm)_2]$ coordination polymer.[25] Intra-chain hydrogen bonding occurs between a hydrogen atom of a coordinated ammonia ligand and an adjacent oxygen atom of an adjacent nitroso group (Table 3, Figure 3, b).

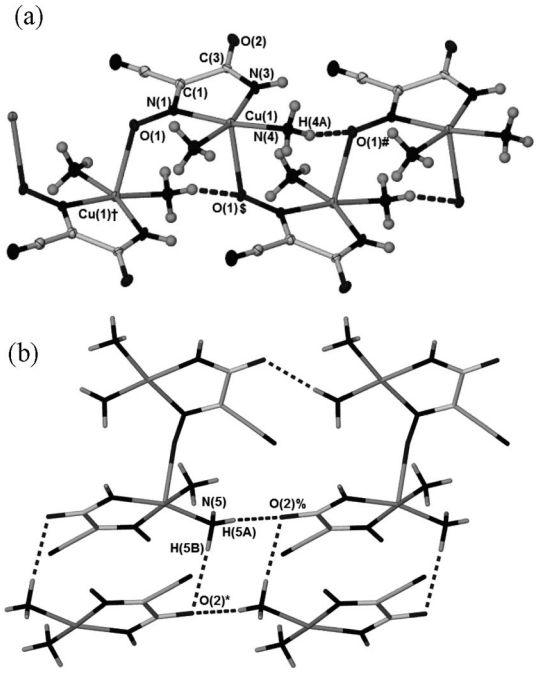

Figure 3. (a) Part of a 1D chain of complex $[Cu(acnm)(NH_3)_2]_\infty$ in the crystal structure of **2**. Ellipsoids shown at 70% probability. Hydrogen bond length and angle: N(4)···O(1)$^{\#}$ 2.967(3) Å; N(4)–H(4A)···O(1)$^{\#}$ 162°. Symmetry elements used: † 3/4 – *x*, 1/2 + *y*, 3/2 – *z*; $^{\#}$ *x*, *y* – 1, *z*; $^{\$}$ 3/2 – *x*, *y* – 1/2, 3/2 – *z*. (b) Intermoleculer hydrogen bonding between 1D chains in **2** resulting in the formation of a 3D network; portions of four chains displayed. Hydrogen bond lengths [Å] and angles [°]: N(5)···O(2)$^{\%}$ 2.968(3); N(5)–H(5A)···O(2)$^{\%}$ 174; N(5)···O(2)* 3.166(3); N(5)–H(5B)···O(2)* 163. Symmetry elements used: * 2 – *x*, 2 – *y*, 2 – *z*; $^{\%}$ *x* – 1, *y*, *z*.

Intermolecular hydrogen bonding results in the formation of a 3D hydrogen-bonded network. The hydrogen atoms of one of the coordinated ammonia ligands form hydrogen bonds to the oxygen atoms of neighbouring carbonyl groups which act as bifurcated hydrogen-bond acceptors (Figure 3, b). The non-hydrogen-bonding hydrogen atoms of the ammonia ligands are directed into the lattice and do not obviously interact with the nitrile groups.

Table 3. Selected bond lengths [Å] and angles [°] of complex **2**.[a]

Cu(1)···Cu(1)†	4.4274(7)	N(1)–Cu(1)–N(3)	80.9(1)
Cu(1)–N(1)	2.051(2)	N(4)–Cu(1)–N(5)	94.2(1)
Cu(1)–N(3)	1.950(2)	O(1)–N(1)–Cu(1)	127.5(2)
Cu(1)–N(4)	2.021(2)	Cu(1)†–O(1)–N(1)	117.5(1)
Cu(1)–N(5)	1.950(2)	O(1)–N(1)–C(1)	120.4(2)
O(1)–Cu(1)†	2.372(2)	N(3)–C(3)–O(2)	129.7(2)
N(1)–O(1)	1.301(3)	O(1)$^{\$}$–Cu(1)–N(1)	96.0(1)
C(1)–N(1)	1.307(3)	O(1)$^{\$}$–Cu(1)–N(3)	100.2(1)
N(3)–C(3)	1.322(3)	C(3)–O(2)	1.253(3)

[a] Symmetry elements used: † 3/2 – *x*, 1/2 + *y*, 3/2 – *z*; $^{\$}$ 3/2 – *x*, *y* – 1/2, 3/2 – *z*.

Complex $[Cu(acnm)(NH_3)_2(py)]$ (**3**) crystallises in the space group *Pbca* with the complex containing two *cis* ammonia ligands and one chelating acnm ligand occupying the equatorial positions of the square pyramidal copper atom, similar to the coordination environment of the copper atom in **2**, but now a pyridine molecule coordinates in the Jahn–Teller distorted axial position (Figure 4, a, Table 4). Although complexes **2** and **3** are similar in colour they crystallise in discernibly different morphologies and the purity was established by elemental analyses. The pyridine blocks the coordination site from being bridged by adjacent acnm ligands as in **2**, eliminating the possibility of forming a coordination polymer. Intramolecular hydrogen bonding occurs between the hydrogen atom of a coordinated ammonia ligand and the oxygen of the nitroso group of the acnm ligand to form a five-membered ring (Figure 4, a).

Intermolecular hydrogen bonding results in the formation of a 3D network (Figure 4, b). The oxygen atoms of the carbonyl groups act as trifurcated hydrogen-bond acceptors from the hydrogen atoms of three ammonia ligands. The oxygen atom of the nitroso group is a bifurcated hydrogen-bond acceptor, bonding to the hydrogen atoms of an ammonia ligand (intra) and the amido group (inter) of an acnm ligand.

Due to the delocalisation of charge on pseudohalides and related ligands it can be difficult to accurately assign the bond orders of the ligands. The naming of acnm suggests the second anionic charge is located in the nitrogen atom of the amidocarbonyl group. The alternative is the negative charge being located on the oxygen atom to form a imidate group. Examination of the bond lengths from the crystal structures of **1**–**3** did not provide a clear determination of bond order. However, the infrared spectra of complexes **1** and **3** indicate the charge is delocalised over the $CONH^-$ functional group. Peaks at 1592 cm^{-1} and 1580 cm^{-1} for **1** and **3**, respectively, are assigned to ν(CO) and are shifted from the higher wavenumbers expected for a carbonyl group.

The mononuclear complex $[Cu(cenm)_2(H_2O)_2]$ (**4**) crystallises in the space group $P\bar{1}$, with the asymmetric unit containing one half of the metal complex (Figure 5). As frequently observed with ligands resulting from the nucleo-

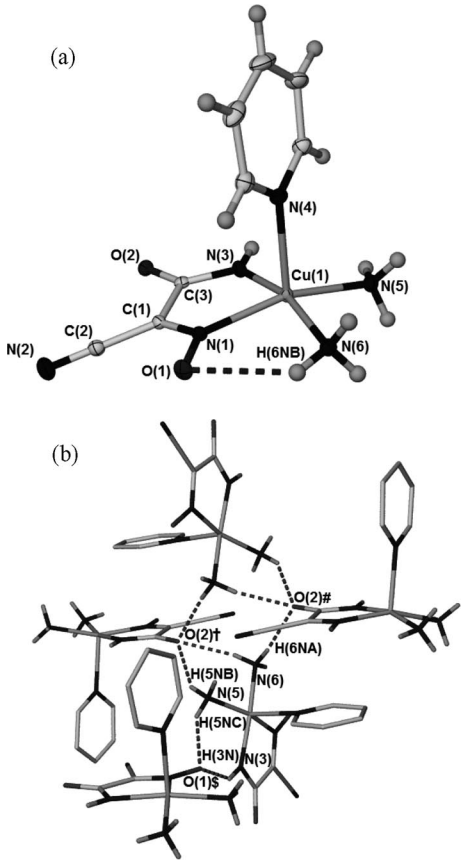

Figure 4. (a) The discrete complex and intramolecular hydrogen bonding in the crystal structure of [Cu(acnm)$(NH_3)_2$(py)] (**3**). Ellipsoids shown at 50% probability. N(6)···O(1) 2.904(2) Å, N(6)–H(6NB)···O(1) 131.2(14). (b) Intermolecular hydrogen bonding in the crystal structure of **3**. Hydrogen atoms of pyridine ligands omitted for clarity. Symmetry elements used: † *x*, 1/2 – *y*, 1/2 + *z*; # 1 – *x*, *y* – 1/2, 1/2 – *z*; $ *x* – 1/2, *y*, 1/2 – *z*.

Table 4. Selected bond and hydrogen bond lengths [Å] and angles [°] in the crystal structure of complex **3**.[a]

Cu(1)–N(1)	2.029(1)	N(1)–Cu(1)–N(3)	80.91(4)
Cu(1)–N(3)	1.960(1)	N(5)–Cu(1)–N(6)	94.74(5)
Cu(1)–N(4)	2.253(1)	N(3)–Cu(1)–N(5)	94.96(5)
Cu(1)–N(5)	2.038(1)	N(1)–Cu(1)–N(4)	99.59(4)
Cu(1)–N(6)	2.002(1)	N(5)–Cu(1)–N(4)	99.34(5)
N(1)–O(1)	1.290(1)	N(6)–Cu(1)–N(4)	97.65(4)
N(1)–C(1)	1.313(2)	O(1)–N(1)–C(1)	121.6(1)
N(3)–C(3)	1.307(2)	N(3)–C(3)–O(2)	129.2(1)
C(3)–O(2)	1.264(2)		
N(3)···O(1)$	2.989(1)	N(3)–H(3N)···O(1)$	141(1)
N(5)···O(1)$	2.956(2)	N(5)–H(5NC)···O(1)$	149(1)
N(5)···O(2)†	3.000(2)	N(5)–H(5NB)···O(2)†	148(1)
N(6)···O(2)†	3.026(2)	N(6)–H(6NC)···O(2)†	160(11)
N(6)···O(2)#	2.942(2)	N(6)–H(6NA)···O(2)#	169(1)

[a] Symmetry elements used: † *x*, 1/2 – *y*, 1/2 + *z*; # –*x*, *y* – 1/2, 1/2 – *z*; $ *x* – 1/2, *y*, 1/2 – *z*.

philic addition of alcohol to dcnm, the cenm chelates to the equatorial positions of the metal centre through the nitrogen atoms of the nitroso and imine groups, with water coordinating in the Jahn–Teller distorted axial positions.

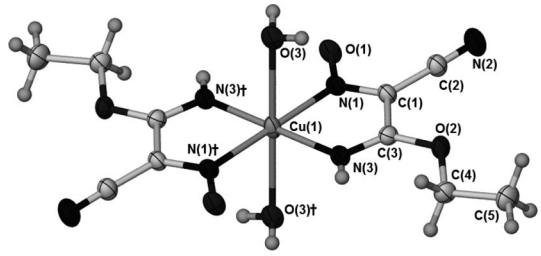

Figure 5. The discrete complex [Cu(cenm)$_2$(H_2O)$_2$] (**4**). Symmetry element used: † –*x*, 2 – *y*, –*z*. Selected bond lengths: Cu(1)–N(1) 2.0551(14); Cu(1)–N(3) 1.9651(15); Cu(1)–O(3) 2.4942(15); N(1)–O(1) 1.279(2); C(1)–N(1) 1.316(2); C(3)–N(3) 1.270(2); C(3)–O(2) 1.325(2) N(1)–Cu(1)–N(3) 80.61(6).

The coordination polymer {[Cu(cenm)$_2$]$_2$·H_2O}$_\infty$ (**5**), crystallises in the space group *C*2/*c*, with the asymmetric unit containing a [Cu(cenm)$_2$] moiety and half a molecule of water. Two cenm ligands chelate equatorially to the central octahedral copper atom, coordinating via the nitrogen atoms of the nitroso group and the imine group. The oxygen atom on the nitroso group of one ligand displays a Jahn–Teller distorted axial bond to a neighbouring [Cu(cenm)$_2$] moiety forming a [Cu(cenm)$_2$]$_2$ unit. This ligand has an out-of-plane μ_2-η^2(N,N′)Cu:η^1(O)Cu′ coordination mode, as observed in the coordination polymer [Cu(cmnm)$_2$][25] and for the acnm ligand of complex **2**. The other unique cenm ligand of the [Cu(cenm)$_2$] moiety has a μ_2-η^2(N,N′)Cu:η^1(N′′)Cu′ coordination mode. This cenm ligand chelates to a copper atom and then bridges through the *nitrile* group to an adjacent [Cu(cenm)$_2$]$_2$ unit into the axial position of the copper atom (Figure 6, a, Table 5). While dcnm has been shown to coordinate through its nitrile groups,[9–11,13] it occurs less frequently with derivative ligands resulting from alcohol addition. Here coordination through the nitrile group facilitates the formation of a 2D sheet with a (4,4) topology (Figure 6, b), with copper dimer nodes. The sheets interdigitate, with ethyl groups of each sheet directed into the cavities of an adjoining sheet (and vice versa).

One water molecule resides in each cavity between [Cu(cenm)$_2$]$_2$ units, acting as a hydrogen-bond donor to the oxygen atoms of coordinating nitroso groups and as a hydrogen-bond acceptor from imino groups. This cross-links the sheets into a 3D α-Po network. Further hydrogen bonding exists between oxygen atoms of the uncoordinated nitroso groups and the imino NH groups (Figure 6, c).

The presence of two crystallographically unique ligands allows a comparison of their different bonding modes and their effects on bond lengths. The ligand with the μ_2:η^2(N,N′)Cu-η^1(O)Cu′ coordination mode has a bond length between nitrogen and oxygen atoms of the nitroso group [N(1)–O(1)] of 1.287(2) Å, marginally longer than the nitroso group of the other cenm ligand [N(4)–O(3)] which has a bond length of 1.261(2) Å. This difference can be attributed to the electron density being drawn away from the bond to coordinate to the copper atom as it adopts some character of an oximate group. The former bond is also

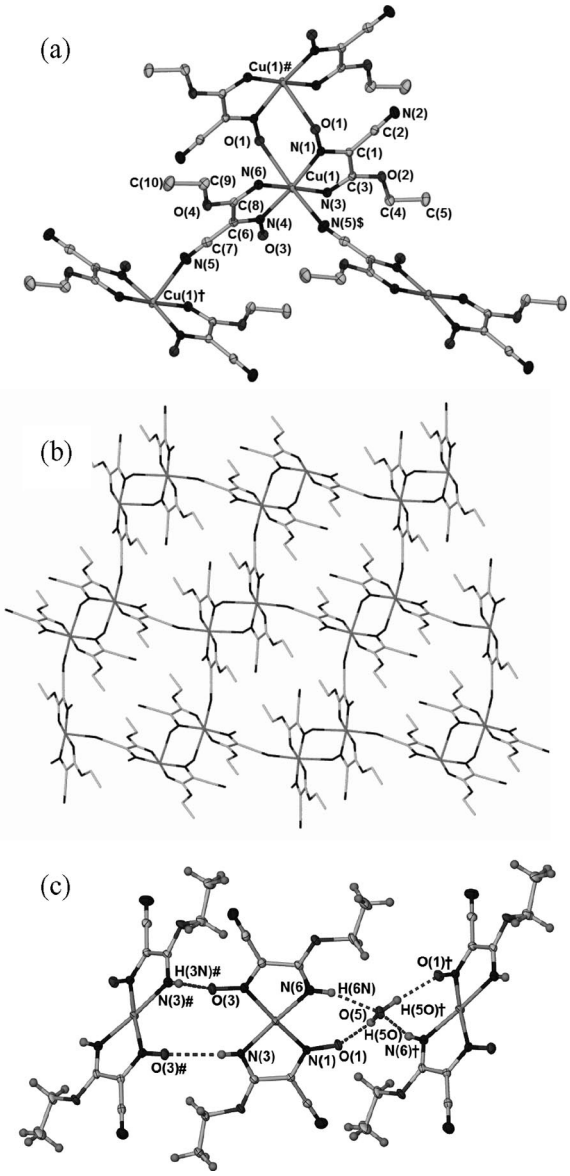

Figure 6. (a) Crystal structure of {[Cu(cenm)$_2$]$_2$·H$_2$O} (**5**). Ellipsoids at 50% probability, water molecule and hydrogen atoms omitted for clarity. Symmetry elements used: † x, 1 – y, z – 1/2; # 3/2 – x, 1/2 – y, 2 – z; $ x, –y, 1/2 + z. (b) (4,4) Topology of the coordination polymer **5**, hydrogen atoms and water molecule omitted for clarity. (c) Hydrogen bonding within **5**. Key hydrogen bond lengths [Å] and angles [°]: N(6)···O(5) 2.867(2); N(6)–H(6N)···O(5) 161(2); O(5)···O(1) 2.727(1); O(5)–H(5O)···O(1) 160(3); N(3)···O(3)# 3.070(2); N(3)–H(3N)···O(3)# 177(2). Symmetry elements used: † 2 – x, y, 5/2 – z; # 1 – x, y, 3/2 – z.

Table 5. Selected bond lengths [Å] and angles [°] of complex **5**.[a]

Cu(1)···Cu(1) †	7.6427(3)	Cu(1)···Cu(1)#	4.3830(4)
Cu(1)–N(1)	2.035(1)	N(1)–Cu(1)–N(3)	81.96(6)
Cu(1)–N(3)	1.974(2)	N(4)–Cu(1)–N(6)	81.89(6)
Cu(1)–N(4)	2.018(1)	N(1)–Cu(1)–N(4)	172.94(5)
Cu(1)–N(6)	1.953(2)	N(6)–Cu(1)–N(3)	176.18(6)
Cu(1)–O(1)#	2.660(1)	N(1)–Cu(1)–N(5)$	88.98(6)
Cu(1)†–N(5)	2.477(2)	N(1)–Cu(1)–O(1)#	84.85(5)
N(1)–O(1)	1.287(2)	N(3)–Cu(1)–N(5)$	84.91(6)
N(1)–C(1)	1.313(2)	N(3)–Cu(1)–O(1)#	98.02(5)
C(1)–C(2)	1.429(2)	O(1)#–Cu(1)–N(5)$	172.72(5)
C(2)–N(2)	1.140(2)	O(1)–N(1)–Cu(1)	129.86(10)
N(3)–C(3)	1.278(2)	C(7)–N(5)–Cu(1)†	162.57(15)
O(2)–C(3)	1.321(2)	O(1)–N(1)–C(1)	119.46(13)
N(4)–O(3)	1.261(2)	O(3)–N(4)–C(6)	121.01(14)
N(4)–C(6)	1.336(2)	N(3)–C(3)–O(2)	130.65(16)
C(6)–C(7)	1.420(2)	N(6)–C(8)–O(4)	128.53(16)
C(7)–N(5)	1.142(2)		
N(6)–C(8)	1.276(2)		
O(4)–C(8)	1.324(2)		

[a] Symmetry elements used: † x, 1 – y, z – 1/2; # 3/2 – x, 1/2 – y, 2 – z; $ x, 1 – y, 1/2 + z.

associated with a shorter C–N(O) bond [1.313(2) Å] than the latter bond as it develops some more C=N character. Interestingly the coordinating nitrile group has no distinguishable change in bond length in comparison to the non-coordinating nitrile group [1.142(2) and 1.140(2) Å respectively]. The infrared spectrum also does not allow for differentiation of the nitrile groups, with only one peak at 2224 cm^{-1} attributable to a nitrile group, although this is clearly at a higher wavenumber than the corresponding peak in the infrared spectrum of **4** at 2207 cm^{-1}.

The $\chi_M T$ data for **5**, per Cu, are plotted as a function of temperature in Figure 2, b. $\chi_M T$ values remain constant at 0.41 cm^3 mol^{-1} K (1.82 μ_B) between 300 and ≈ 10 K, then decrease to reach 0.31 cm^3 mol^{-1} K (1.57 μ_B) at 2 K. The corresponding χ_M vs. T data follow a Curie–Weiss dependence with C = 0.42 cm^3 mol^{-1} K and θ = –0.01 K (Figure 2, b). Clearly, any antiferromagnetic coupling within the nitroso-bridged Cu$_2$ dinuclear moieties is extremely weak and this is not surprising because bridging is through the Cu(1)–N(1){equatorial}O(1){apical}–Cu(1)# pathways (Figure 6, a) that involve Cu($d_{x^2-y^2}$) – O,N(p) – Cu(d_{z^2}) overlap. The other possible coupling, via Cu(1)–N(5)$(nitrile) apical pathways, is negligible. Fitting to a S = 1/2 dimer ($-2J\mathbf{S_1}\cdot\mathbf{S_2}$) model[36] gave best-fit values of g = 2.12, $2J$ = –1.3 cm^{-1}, Na = 65 × 10^{-6} cm^3 mol^{-1}.

The coordination polymer {[Mn$_3$(ccnm)$_2$(EtOH)$_2$(OAc)$_4$]·2EtOH}$_\infty$ (**6**) is a 1D chain and the crystals adopt the space group $P\bar{1}$ (Figure 7, a, Table 6). The repeating unit contains two equivalent seven coordinate manganese atoms and halves of two equivalent six coordinate manganese atoms. The two unique acetate ligands display μ_2-:η^2(O,O′)Mn-η^1(O′)Mn′ and μ_2-η^1(O)Mn:η^1(O′)Mn′ bridging coordination modes. The μ_3-η^1(O)Mn:η^2(N,O′)Mn′:η^1(O′)Mn′′ bonding (Figure 7, b) has not previously been observed for the ccnm ligand. The coordination sphere of the seven coordinate manganese atoms contains a bidentate ccnm ligand, two bridging acetate ligands (binding η^2 and η^1), one ethanol and a ccnm ligand from an adjacent unit, bridging via the oxygen atom of the carbamoyl group. The coordination sphere of the six coordinate manganese atoms contain two trans ccnm ligands, which coordinate via the oxygen atoms of the nitroso group, and four acetate ligands (two unique) that display η^1 coordination to the metal centre in a trans array.

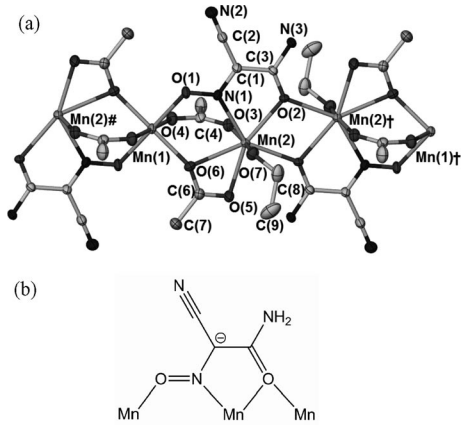

Figure 7. (a) Crystal structure of a portion of the polymeric chain in $\{[Mn^{II}_3(ccnm)_2(EtOH)_2(OAc)_4]\cdot 2EtOH\}_\infty$ (**6**), non-coordinated ethanol molecules and hydrogen atoms omitted for clarity. Ellipsoids shown at 50% probability. Symmetry element used: † $1-x$, $1-y$, $1-z$. (b) The μ_3-η^1O(Mn):η^2N,O′(Mn′):η^1O′(Mn′′) coordination mode of ccnm.

Table 6. Selected bond lengths [Å] and angles [°] of complex **6**.[a]

Mn(1)···Mn(2)	3.7341(9)	Mn(2)···Mn(2) †	3.7635(14)
Mn(1)–O(1)	2.168(3)	O(1)–Mn(1)–O(6)	87.5(1)
Mn(1)–O(4)	2.193(3)	O(1)–Mn(1)–O(4)	93.0(1)
Mn(1)–O(6)	2.130(2)	O(4)–Mn(1)–O(6)	90.8(1)
Mn(2)–N(1)	2.330(2)	O(1)–Mn(1)–O(1)#	180.0(1)
Mn(2)–O(2)	2.335(3)	N(1)–Mn(2)–O(2)	141.4(1)
Mn(2)–O(3)	2.111(3)	O(6)–Mn(2)–O(5)	55.1(1)
Mn(2)–O(5)	2.251(3)	O(3)–Mn(2)–O(7)	165.7(1)
Mn(2)–O(6)	2.435(3)	O(2)–Mn(2)–O(7)	88.3(1)
Mn(2)–O(7)	2.172(3)	O(5)–Mn(2)–O(3)	92.0(1)
Mn(2)†–O(2)	2.289(2)	Mn(1)–O(6)–Mn(2)	109.6(1)
N(1)–O(1)	1.291(4)	Mn(2)–O(2)–Mn(2)†	109.0(1)
N(1)–C(1)	1.320(4)	N(1)–O(1)–Mn(1)	116.9(2)
O(2)–C(3)	1.259(4)	O(1)–N(1)–Mn(2)	126.8(2)
C(3)–N(3)	1.322(4)	O(1)–N(1)–C(1)	117.5(3)
C(2)–N(2)	1.139(5)	O(2)–C(3)–N(3)	123.5(3)

[a] Symmetry elements used: † $1-x$, $1-y$, $1-z$; # $1-x$, $1-y$, $-z$.

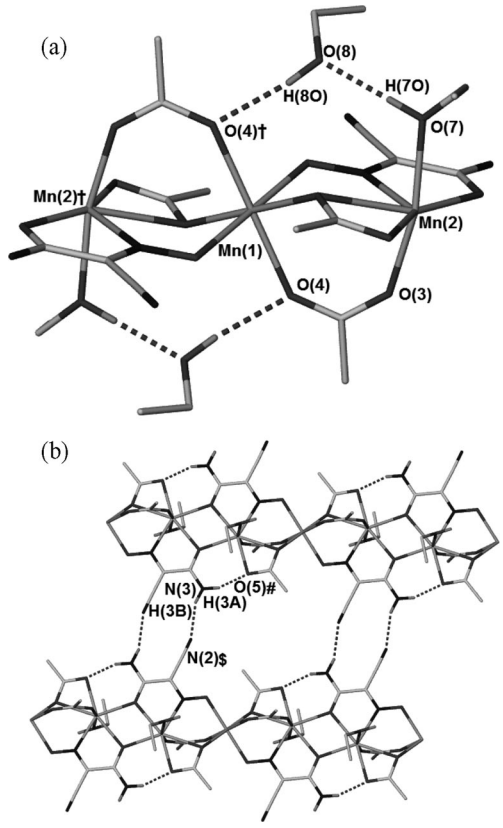

Figure 8. (a) Hydrogen bonding between lattice and coordinated ethanol molecules in **6**. (b) Hydrogen bonding with the amino group acting as the hydrogen-bond donor. Non-hydrogen-bonding hydrogen atoms omitted for clarity. Symmetry elements used: † $1-x$, $1-y$, $-z$; # $1-x$, $1-y$, $1-z$; $ $2-x$, $2-y$, $1-z$. Key hydrogen bond lengths [Å] and angles [°]: O(7)···O(8) 2.693(4); O(7)–H(7O)···O(8) 179(6); O(8)···O(4) 2.860(4); O(8)–H(8O)···O(4) 164(4); N(3)···N(2)$ 2.993(4); N(3)–H(3B)···N(2)$ 159.9; N(3)···O(5)# 2.668(4); N(3)–H(3A)···O(5)# 154.4.

Two types of hydrogen bonding are observed along the 1D chain; the oxygen of the coordinating ethanol ligand acts as a hydrogen-bond donor to the ethanol molecule in the lattice. This in turn acts as a hydrogen-bond donor to the oxygen atom of the acetate molecule which bridges between Mn(1) and Mn(2) with a μ_2:η^1-η^1 coordination mode (Figure 8, a). Intra-chain hydrogen bonding occurs between the amine group of the ccnm ligand and the adjacent bridging acetate ligand which bridges between manganese atoms with a μ_2:η^2-η^1 coordination mode. The formation of hydrogen-bonded 2D sheets results from the other hydrogen atom of the amine group hydrogen bonding to the nitrile group of a ccnm ligand from a neighbouring chain (Figure 8, b).

Complex $(Et_4N)_2[Cu(ccnm)_4]$ (**7**), crystallises in the space group $P2_1/n$ with the asymmetric unit containing one unique half of the complex. Two of the ccnm ligands exhibit the usual bidentate chelation via the nitrogen and oxygen atoms of the nitroso and carbamoyl groups, respectively, to the equatorial positions of the octahedral copper. The other two ccnm ligands coordinate to the Jahn–Teller distorted axial positions of the metal centre through the nitrogen atoms of their *nitrile* groups. To the best of our knowledge this is the only example of η^1 nitrile coordination observed for a derivative of the dcnm ligand (Figure 9, Table 7). This is in contrast to the more normal behaviour of dcnm in a sterically crowded environment around a transition metal, where it often exhibits an η^1 coordination through the oxygen atom[30,31] or the nitrogen atom[15,37] of the nitroso group.

Complex **7** is highly unusual as it is one of the few discrete complexes in which the coordination sphere of the d-block metal is completely filled by dcnm derived ligands and not by additional co-ligands or solvent molecules. Previous examples with relevant ligands included $[Co^{III}(mici)_3]$ (mici = dimethylimidodicarbonimidate),[38] where mici is the result of the addition of methanol to both nitrile arms of dca. $(Et_4N)_2[Cu(ccnm)_4]$ is the only discrete complex to have four addition product ligands coordinated to the metal centre, albeit two being bidentate and two unidentate.

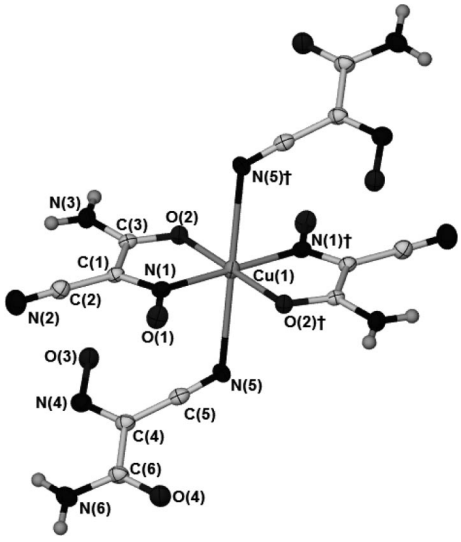

Figure 9. The $[Cu(ccnm)_4]^{2-}$ anion in the crystal structure of **7**. Ellipsoids shown at 50% probability. Symmetry element used: † 1 – *x*, –*y*, –*z*.

Table 7. Selected bond lengths [Å] and angles [°] of complex **7**.[a]

Cu(1)–N(1)	1.973(2)	N(1)–Cu(1)–O(2)	83.3(1)
Cu(1)–O(2)	1.955(2)	N(1)–Cu(1)–N(5)	82.7(7)
Cu(1)–N(5)	2.654(2)	O(2)–Cu(1)–N(5)	95.9(6)
N(1)–O(1)	1.265(2)	N(1)–Cu(1)–O(2)†	96.8(1)
N(1)–C(1)	1.328(3)	C(5)–N(5)–Cu(1)	119.8(2)
N(2)–C(2)	1.143(3)	O(1)–N(1)–C(1)	121.5(2)
O(2)–C(3)	1.268(3)	O(2)–C(3)–N(3)	121.9(2)
N(3)–C(3)	1.306(3)	C(1)–C(2)–N(2)	178.6(2)
N(4)–O(3)	1.281(2)	O(3)–N(4)–C(4)	117.9(2)
N(4)–C(4)	1.332(3)	O(4)–C(6)–N(6)	123.8(2)
N(5)–C(5)	1.156(3)	C(4)–C(5)–N(5)	175.9(2)
O(4)–C(6)	1.239(3)		
N(6)–C(6)	1.335(3)		

[a] Symmetry element used: † 1 – *x*, –*y*, –*z*.

As with complex **5**, the presence of two crystallographically unique ccnm ligands within the crystal structure of **7** (Figure 10) allows for comparison of different coordination modes and their effect on bond lengths. Although the ligand coordinating through the nitrile group may show a lengthening of the C≡N bond [1.156(3) Å] in comparison to the non-coordinating nitrile group [1.143(3) Å], the difference is within 3σ, thus prohibiting any definitive distinction between the two. However, the infrared spectra has two ν(CN) peaks at 2218 cm^{-1} and 2189 cm^{-1} which would correspond to the two different nitrile groups.

Complex $[Mn(cmnm)_3Mn(bipy)(MeOH)](ClO_4)$ (**8**), crystallises in the space group $P2_1/m$ and contains the $[Mn^{II}(cmnm)_3]^-$ moiety observed in the $[Mn^{III}Mn^{II}_2(cmnm)_6](NO_3)$ complex.[12] It is similar to the $[Ni(ccnm)_3]^-$ analogue within $[Na(H_2O)_6][NaNi_2(ccnm)_6]$.[14] In the metalloligand the octahedral manganese atom is chelated by three cmnm ligands, two of which are crystallographically unique, and is bridged to the other manganese atom via the nitroso group with a μ_2-η^1N(Mn):η^1O(Mn′) coordination mode (Figure 11, Table 8). The other manganese atom is also octahedral and has its coordination sphere completed by a

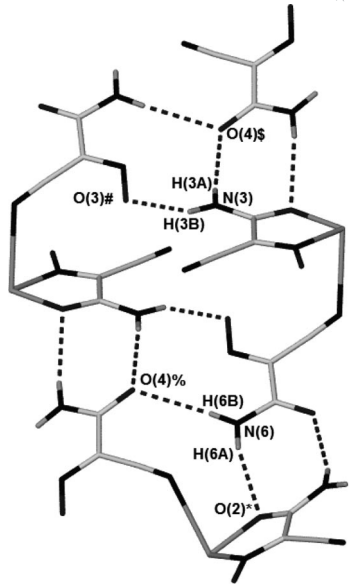

Figure 10. Hydrogen bonding between $[Cu(ccnm)_4]^{2-}$ ions, within the crystal structure of **7**, tetraethylammonium counter-cations omitted for clarity. Symmetry elements used: $ *x* – 1/2, 1/2 – *y*, *z* – 1/2; # 1 – *x*, 1 – *y*, –*z*; * 1/2 + *x*, 1/2 – *y*, 1/2 + *z*; % 3/2 – *x*, 1/2 + *y*, 1/2 – *z*. Key hydrogen bond lengths [Å] and angles [°]: N(3)···O(4)$ 2.934(2); N(3)–H(3A)···O(4)$ 151.6; N(3)···O(3)# 2.777(3); N(3)–H(3B)···O(3)# 151.5; N(6)···O(2)* 3.137(2); N(6)–H(6A)···O(2)* 158.8; N(6)···O(4)% 3.266(3); N(6)–H(6B)···O(4)% 149.1.

bipy ligand and a methanol molecule, in addition to the three oxygen atoms of the nitroso groups. The configuration of the nitrogen atoms of the imino groups are ideally situated for hydrogen bonding to the perchlorate anion which "docks" into the "back end" of the $[Mn(cmnm)_3]^-$ moiety. The crystal structure reveals extensive disorder of methanol solvent contained within the lattice.

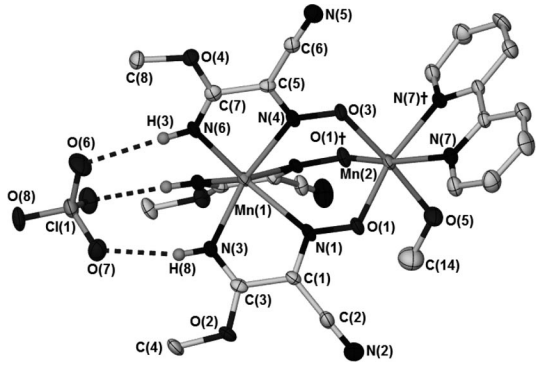

Figure 11. The complex $[Mn(cmnm)_3Mn(bipy)(MeOH)](ClO_4)$ from within the crystal structure of **8**·3.4MeOH. Non-hydrogen-bonding atoms omitted for clarity, ellipsoids shown at 50% probability. Symmetry element used: † *x*, 1/2 – *y*, *z*. Hydrogen bond lengths [Å] and angles [°]: N(6)···O(6) 3.194(6); N(6)–H(3)···O(6) 164(5); N(3)···O(7) 3.033(4); N(3)–H(8)···O(7) 168(4).

The plot of molar susceptibility, $\chi_M T$ per Mn, vs. temperature is given for complex **8** in Figure 12. The $\chi_M T$ values decrease gradually, from 4.14 $cm^3 mol^{-1} K$ at 300 K (5.94 μ_B per Mn), to ca. 3.2 $cm^3 mol^{-1} K$ (5.06 μ_B) at 50 K, reaching 0.36 $cm^3 mol^{-1} K$ (1.7 μ_B) at 2 K. The correspond-

Table 8. Selected bond lengths [Å] and angles [°] of complex **8**.[a]

Mn(1)···Mn(2)	3.9152(15)		
Mn(1)–N(1)	2.354(3)	N(1)–Mn(1)–N(3)	129.6(1)
Mn(1)–N(3)	2.212(3)	N(4)–Mn(1)–N(6)	73.3(2)
Mn(1)–N(4)	2.294(4)	N(1)–Mn(1)–N(4)	83.6(1)
Mn(1)–N(6)	2.194(4)	N(3)–Mn(1)–N(6)	95.0(1)
Mn(2)–O(1)	2.125(2)	N(1)–Mn(1)–N(1)†	84.0(2)
Mn(2)–O(3)	2.157(3)	O(1)–Mn(2)–O(3)	92.4(1)
Mn(2)–O(5)	2.234(4)	O(1)–Mn(2)–N(7)	93.5(1)
Mn(2)–N(7)	2.247(3)	O(1)–Mn(2)–O(5)	84.8(1)
N(1)–O(1)	1.315(3)	N(7)–Mn(2)–N(7)†	72.4(2)
N(1)–C(1)	1.309(4)	Mn(1)–N(1)–O(1)	130.8(2)
N(3)–C(3)	1.267(5)	Mn(1)–N(4)–O(3)	129.5(3)
C(3)–O(2)	1.342(4)	N(1)–O(1)–Mn(2)	119.8(2)
N(4)–O(3)	1.299(5)	O(1)–N(1)–C(1)	115.9(3)
N(4)–C(5)	1.323(6)	N(3)–C(3)–O(2)	129.0(3)
N(6)–C(7)	1.267(6)	O(3)–N(4)–C(5)	117.2(4)
O(4)–C(7)	1.335(6)	N(6)–C(7)–O(4)	129.2(5)

[a] Symmetry element used: † x, 1/2 – y, z.

ing plot of χ_M shows a maximum at 10 K indicative of weak antiferromagnetic coupling occurring across the triply bridging Mn–NO–Mn pathways. Fitting to a S = 5/2 Heisenberg $-2J\mathbf{S_1}\cdot\mathbf{S_2}$ dimer model gave best-fit parameter values of g = 1.99, J = –1.44 cm^{-1}. In the many studies reported of triply bridging oximate species, usually heterodinuclear or heterotrinuclear in character, and often employing pyridinealdoximates[39] as bridging groups (analogous to cmnm in **7**), the $d^5 - d^5$ combination could not be observed for a comparison to be made of J values. The orbital overlap arguments put forward previously[33,39,40] when applied to the $t_{2g}^3e_g^2 - t_{2g}^3e_g^2$ combination, would predict weak antiferromagnetic coupling, as observed here.

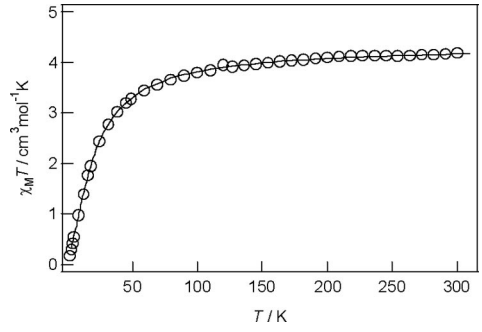

Figure 12. Plot of $\chi_M T$, per Mn, for complex **8**. The solid line is the calculated plot using the parameters given in the text.

Complex [Mn(bipy)$_2$(dcnm)$_2$] (**9**) crystallises from solution in the space group $P\bar{1}$. The complex consists of an octahedral manganese atom coordinated by two bidentate bipy ligands and two dcnm ligands with an η^1 coordination through the oxygen atom of the nitroso group (Figure 13, Table 9).

Complexes [Mn(bipy)$_2$(dcnm)(H$_2$O)](dcnm)·H$_2$O (**10**) and [Mn(bipy)$_2$(dcnm)(H$_2$O)](dcnm) (**11**) cocrystallise from the same reaction mixture and contain the same cationic [Mn(bipy)$_2$(H$_2$O)(dcnm)]$^+$ complex. The free dcnm counterion in the lattice is disordered over two positions and acts as a hydrogen-bond acceptor to the hydrogen bond

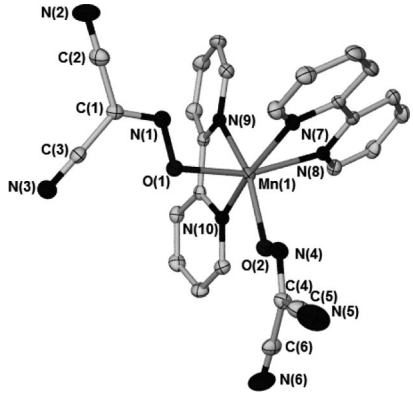

Figure 13. The complex [Mn(bipy)$_2$(dcnm)$_2$] in the crystal structure of **9**. Ellipsoids shown at 50% probability, hydrogen atoms omitted for clarity.

Table 9. Selected bond lengths [Å] for complex **9**.

Mn(1)–O(1)	2.159(1)	C(3)–N(3)	1.142(2)
Mn(1)–O(2)	2.129(1)	O(2)–N(4)	1.303(2)
Mn(1)–N(7)	2.239(1)	N(4)–C(4)	1.315(2)
Mn(1)–N(8)	2.267(1)	C(4)–C(5)	1.431(2)
Mn(1)–N(9)	2.274(1)	N(1)–O(1)	1.304(2)
Mn(1)–N(10)	2.289(1)	N(1)–C(1)	1.317(2)
N(1)–O(1)	1.304(2)	C(5)–N(5)	1.144(2)
N(1)–C(1)	1.317(2)	C(4)–C(6)	1.435(2)
C(1)–C(2)	1.428(2)	C(6)–N(6)	1.140(2)
C(2)–N(2)	1.141(2)		

from the water ligands coordinating to the manganese atom (Figure 14, Table 10). Due to the similar colour and morphology of the crystals, manual separation was not possible. Elemental analysis indicates that washing the product with methanol and ether results in the complete removal of lattice water of **10** and the partial removal of water coordinated to the manganese atom.

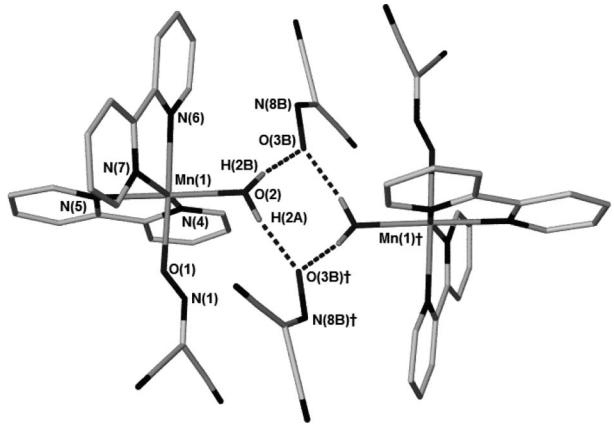

Figure 14. The complex [Mn(bipy)$_2$(dcnm)(H$_2$O)](dcnm) in the crystal structure of **11**. Non-hydrogen-bonding hydrogen atoms and one disordered position of the dcnm ligand removed for clarity. Hydrogen bond lengths [Å] and angles [°]: O(2)···O(3B) 2.600(5); O(2)–H(2B)···O(3B) 169(4); O(2)···O(3B)† 2.702(6); O(2)–H(2A)···O(3B)† 155(4). Symmetry element used: † 2 – x, 1 – y, 2 – z. This structure is also representative of complex **10**.

Table 10. Selected bond lengths [Å] for complex **11**. Values also representative of complex **10**.[a]

Mn(1)–O(1)	2.146(2)	O(1)–Mn(1)–O(2)	91.9(1)
Mn(1)–O(2)	2.168(2)	O(1)–Mn(1)–N(4)	93.7(1)
Mn(1)–N(4)	2.240(2)	O(1)–Mn(1)–N(6)	165.0(1)
Mn(1)–N(5)	2.279(2)	O(2)–Mn(1)–N(7)	95.6(1)
Mn(1)–N(6)	2.258(2)	O(2)–Mn(1)–N(4)	95.6(1)
Mn(1)–N(7)	2.237(2)	O(2)–Mn(1)–N(5)	170.0(1)
O(1)–N(1)	1.307(2)	N(1)–O(1)–Mn(1)	115.1(2)

[a] Symmetry element used: † 2 – *x*, 1 – *y*, 2 – *z*.

Complex $[Cu(cgnm)_2(H_2O)_2]$ (**12**), crystallises in the space group $P\bar{1}$ with half the complex contained within the asymmetric unit (Figure 15, a). Typical of complexes of this type, the Jahn–Teller distorted copper metal centre has its coordination sphere comprised of two trans equatorially *N*,*N*′-chelating cgnm ligands with two aqua ligands in the axial positions. The 2-methoxyethoxy chains of the ligands are directed into the lattice and are not involved in coordination. As with complex **4** an examination of the bond lengths within **12** indicate the cgnm ligand has similar bond orders to those observed in other nucleophilic alcohol addition ligands, with N(1)–O(1) and C(1)–N(1) bond lengths of 1.284(2) and 1.317(2) Å, respectively, supporting the determination of a nitroso, rather than oximate, functional group (Table 11).

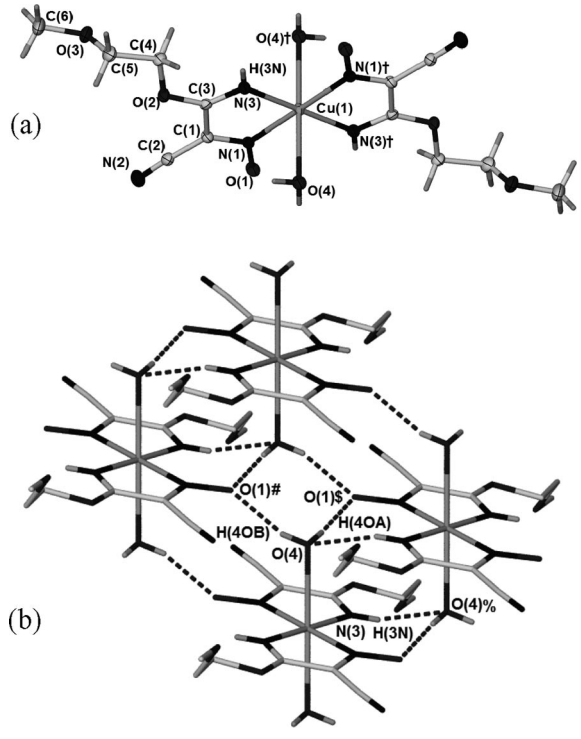

Figure 15. (a) The complex $[Cu(cgnm)_2(H_2O)_2]$ and (b) hydrogen bonding between complex molecules in the crystal structure of **12**. Symmetry elements used: † –*x*, –*y*, –*z*; # –*x*, –*y* – 1, –*z*; $ 1 + *x*, *y*, *z*;% 1 – *x*, –*y*, –*z*. Hydrogen bond lengths [Å] and angles [°]: N(3)···O(4)% 2.832(2); N(3)–H(3N)···O(4)% 149(2); O(4)···O(1)$ 2.708(2); O(4)–H(4OA)···O(1)$ 172(3); O(4)–O(1)# 2.847(2); O(4)–H(4OB)···O(1)# 143(2).

Table 11. Selected bond lengths [Å] for complex **12**.[a]

Cu(1)–N(1)	2.067(1)	N(1)–Cu(1)–N(3)	80.47(5)
Cu(1)–N(3)	1.959(1)	N(1)–Cu(1)–O(4)	81.81(5)
Cu(1)–O(4)	2.477(2)	N(3)–Cu(1)–O(4)	91.88(5)
C(3)–N(3)	1.276(2)	N(3)–Cu(1)–N(1)†	99.53(5)
C(3)–O(2)	1.323(2)	O(4)–Cu(1)–N(1)†	98.19(5)
N(1)–O(1)	1.284(2)	N(3)–C(3)–O(2)	128.73(14)
C(1)–N(1)	1.317(2)	Cu(1)–N(1)–C(1)	111.61(10)

[a] Symmetry element used: † –*x*, –*y*, –*z*.

The hydrogen-bonding network in **12** is the same as that observed in $[Cu(cmnm)_2(H_2O)_2]$,[25] with the oxygen atom of each nitroso group directed into the lattice acting as a hydrogen-bond acceptor, and with the coordinated water of adjacent complexes acting as the hydrogen-bond donor (Figure 15, b). The imine groups act as hydrogen-bond donors to the oxygen atoms of coordinated waters in adjacent complexes, resulting in the formation of hydrogen-bonded 2D sheets.

Conclusions

In this paper we report a range of complexes, coordination polymers and new coordination modes of the derivative ligands resulting from the nucleophilic addition of water or alcohol to dcnm. Complexes **1** to **3** contain the dianionic acnm ligand, which results from the deprotonation of ccnm, with bridging modes through the nitroso group. The crystal structure of $[Cu(cenm)_2(H_2O)_2]$ (**4**) is reported in conjunction with the first instance of the ethanol addition ligand cenm being incorporated into a coordination polymer, namely the complex $\{[Cu(cenm)_2]_2{\cdot}H_2O\}_\infty$ (**5**). This has a different coordination mode for each unique ligand, one of which unusually shows tridentate coordination. The magnetic properties of **5** are consistent with very weak antiferromagnetic coupling which is in contrast to the magnetic data for the trinuclear species **1** for which strong antiferromagnetic coupling occurs, via the double alkoxo-nitroso bridging, leading to a spin ground state of 1/2. The coordination polymer $\{[Mn_3(ccnm)_2EtOH_2(OAc)_4]{\cdot}2EtOH\}_\infty$ (**6**) contains a ccnm with a previously unobserved μ_2 bridging mode through the oxygen atom of a carbamoyl group that facilitates the formation of a 1D chain. The discrete complex $(Et_4N)_2[Cu(ccnm)_4]$ (**7**), synthesised from the preformed $(Et_4N)(ccnm)$, has two ligands with an unusual coordination mode, namely solely through the nitrile group, and has various hydrogen-bonding motifs through the carbamoyl and nitroso functional groups. $[Mn(cmnm)_3Mn(bipy)(MeOH)](ClO_4)$ (**8**) displays weak antiferromagnetic coupling across the three nitroso bridges with a *J* value of –1.44 cm^{-1}, a value anticipated from the magnetic exchange observed in triply-bridged oximato compounds. A change in solvent in these Mn^{II}–dcnm reactions resulted in only mononuclear complexes being isolated with no nucleophilic addition to the nitrile groups of dcnm occurring (compounds **9**–**11**). However, the large alcohol addition ligand cgnm {cyano[imino(2-methoxyethoxy)methyl]nitrosomethanide} in **12** is the result of a copper promoted ad-

dition of ethylene glycol monomethyl ether to dcnm, demonstrating that the nucleophilic addition of alcohols is a general reaction not limited to just small chain alcohols such as methanol or ethanol. More generally, these results demonstrate the existence of a new family of anions that can be obtained through the nucleophilic addition of a range of alcohols to dcnm and other related anions. These anions are remarkably versatile ligands that can show a number of bridging modes between metal centres, and it portends well for their inclusion into higher nuclearity complexes. The heterofunctionalised nature of the ligands derived from nucleophilic addition to dcnm also suggests a future role in the formation of heterometallic complexes. Because oxime groups can bridge manganese atoms in large clusters[40] giving single molecule magnets[41] and single chain magnets,[42] the C–N=O functionality of the present ligand offers scope for building high nuclearity magnetic clusters.

Experimental Section

General: Laboratory reagents and solvents were used as provided commercially. Elemental analyses (C, H, N) were performed by the Campbell Analytical Laboratory, University of Otago, New Zealand. ATR-IR spectra were recorded with a Bruker Equinox 55 series FTIR spectrometer in the range 4000–500 cm^{-1} with a resolution of 4 cm^{-1}. Ag(dcnm),[43] Na(dcnm),[10] (Me_4N)(dcnm)[37] and (Et_4N)(ccnm)[17] were prepared according to literature procedures.

$[Cu_3(acnm)_2(dmae)_2(H_2O)_2]$ (1): Na(dcnm) (30 mg, 256 μmol) and $Cu(ClO_4)_2{\cdot}6H_2O$ (47 mg, 127 μmol) were dissolved in water (4 mL). 2-(Dimethylamino)ethanol (0.1 mL) was added to the reaction solution. Standing for four days yielded blue tabular crystals of the product which were washed with water, methanol and diethyl ether and air-dried overnight (26 mg, 98%). IR (ATR): $\tilde{\nu}$ = 3364 (m), 3232 (m, br), 2971 (w), 2881 (w), 2808 (m), 2220 (w), 1592 (s), 1511 (m), 1482 (sh), 1464 (m), 1400 (m), 1260 (m), 1229 (sh), 1147 (m), 1071 (m), 1027 (m), 952 (w), 788 (sh), 744 (w), 660 (w) cm^{-1}. $C_{14}H_{26}Cu_3N_8O_8$ (625.04): calcd. C 26.90, H 4.19, N 17.93; found C 26.73, H 4.18, N 17.82.

$[Cu(acnm)(NH_3)_2]_\infty$ (2): (Me_4N)(dcnm) (40 mg, 237 μmol) was dissolved in pyridine (4 mL). $Cu(ClO_4)_2{\cdot}6H_2O$ (44 mg, 119 μmol) dissolved in water (1 mL) and 28% aqueous ammonia (0.5 mL) were added to the reaction solution. Deep blue crystals were isolated after two weeks (5 mg, 20%). $C_3H_7CuN_5O_2$ (208.67): calcd. C 17.27, H 3.38, N 33.56; found C 17.50, H 3.40, N 33.54.

$[Cu(acnm)(NH_3)_2(py)]$ (3): (Et_4N)(ccnm) (71 mg, 293 μmol) dissolved water (0.5 mL) was added to $Cu(ClO_4)_2{\cdot}6H_2O$ (55 mg, 148 μmol) in water (0.5 mL). Pyridine (5 mL) and 28% aqueous ammonia (0.6 mL) were added to the reaction solution. Deep blue crystals of product formed over two weeks which were washed with pyridine and air-dried (26 mg, 62%). IR (ATR): $\tilde{\nu}$ = 3337 (s), 3311 (sh), 3223 (s), 3147 (m), 2202 (m), 1635 (w), 1580 (vs), 1571 (sh), 1440 (m), 1398 (m), 1282 (m), 1230 (m), 1215 (m), 1200 (m), 1160 (m), 1035 (w), 1004 (w), 745 (w), 719 (m), 694 (w) cm^{-1}. $C_8H_{12}Cu_1N_6O_2$ (287.77): calcd. C 33.39, H 4.20, N 29.20; found C 33.68, H 4.32, N 29.29.

$[Cu(cenm)_2(H_2O)_2]$ (4): (Me_4N)(dcnm) (50 mg, 297 μmol) and $Cu(NO_3)_2{\cdot}3H_2O$ (24 mg, 99 μmol) were dissolved in ethanol (7 mL). Green needle crystals began to form after one month, and after twenty two months the crystals were filtered from the reaction solution, washed with ethanol and diethyl ether and air-dried (17 mg, 45%). IR (ATR): $\tilde{\nu}$ = 3464 (w, br), 3352 (s), 3266 (w, br), 2995 (w), 2207 (m), 1616 (s), 1414 (m, sh), 1379 (s), 1306 (m, sh), 1146 (s), 1103 (w), 1015 (w), 877 (w), 832 (w), 789 (w), 727 (w), 699 (w) cm^{-1}. $C_{10}H_{16}CuN_6O_6$ (379.82) calcd. C 31.62, H 4.25, N 22.13; found C 32.03, H 4.18, N 22.41.

$\{[Cu(cenm)_2]_2{\cdot}H_2O\}_\infty$ (5): $Cu(NO_3)_2{\cdot}3H_2O$ (23 mg, 95 μmol) and $Gd(NO_3)_3{\cdot}6H_2O$ (51 mg, 113 μmol) dissolved in ethanol (3 mL) were added to Na(dcnm) (40 mg, 341 μmol) dissolved in ethanol (3 mL). After standing for ten weeks the reaction solution yielded green block crystalline product which was washed with water, ethanol and ether and air-dried overnight (21 mg, 31%). IR (ATR): $\tilde{\nu}$ = 3168 (m, br), 3005 (w), 2987 (w), 2224 (m), 1618 (s), 1472 (vw), 1433 (s), 1384 (vs), 1360 (m), 1338 (s), 1290 (s), 1248 (sh), 1199 (vw), 1163 (s), 1148 (s), 1109 (s), 1008 (m), 836 (vw), 797 (m), 722 (vw) cm^{-1}. $C_{20}H_{20}Cu_2N_{12}O_9$ (705.59): calcd. C 34.04, H 3.71, N 23.82; found C 34.03, H 4.02, N 24.06.

$\{[Mn_3(ccnm)_2(EtOH)_2(OAc)_4]{\cdot}2EtOH\}_\infty$ (6): Na(dcnm) (40 mg, 342 μmol) dissolved in ethanol (1 mL) was added to $Mn(OAc)_2{\cdot}4H_2O$ (63 mg, 256 μmol) in an ethanol/water (5:1.5 mL) solution. Small red crystals of **6** formed after three months. Insufficient product could be obtained for further analysis.

$(Et_4N)_2[Cu(ccnm)_4]$ (7): (Et_4N)(ccnm) (71 mg, 293 μmol) in methanol (2 mL) was added to $CuCl_2{\cdot}2H_2O$ (15 mg, 88 μmol) and $LaCl_3{\cdot}7H_2O$ (17 mg, 45 μmol) dissolved in methanol (1 mL). Diethyl ether was slowly diffused into the reaction solution yielding green needle crystals of $(Et_4N)_2[Cu(ccnm)_4]$ in two weeks. The crystals were manually separated from a brown precipitate in a water/methanol solution leading to a slight dissolution of the product, lowering the yield and causing absorption of one molecule of water per copper complex as indicated by elemental analysis (5 mg, 9%). IR (ATR): $\tilde{\nu}$ = 3314 (vw), 2986 (vw), 2218 (m), 2189 (m), 1665 (m), 1630 (s), 1567 (s), 1486 (m), 1440 (w), 1392 (vs), 1392 (w), 1292 (w), 1250 (s), 1195 (w), 1175 (w), 1095 (s), 1061 (m), 1002 (m), 785 (w), 737 (s), 677 (s) cm^{-1}. $C_{28}H_{50}Cu_1N_{14}O_9$ (Metal complex plus one absorbed molecule of water) (790.33) calcd. C 42.55, H 6.38, N 24.81; found C 42.96, H 6.42, N 24.51.

$[Mn(cmnm)_3Mn(bipy)(MeOH)](ClO_4)$ (8): Na(dcnm) (50 mg, 427 μmol) dissolved in methanol (3 mL) was added to $Mn(ClO_4)_2{\cdot}6H_2O$ (57 mg, 213 μmol) dissolved in methanol (2 mL). 2,2′-Bipyridine (33 mg, 211 μmol) dissolved in methanol (1 mL) was added to the reaction solution. After standing for three weeks the reactions solution yielded red tabular crystals (**8**), which were washed with methanol and diethyl ether and left to air-dry overnight (9 mg, 11%). Exposure to the atmosphere resulted in absorption of one molecule of water per two dinuclear complexes, as indicated by elemental analysis. IR (ATR): $\tilde{\nu}$ = 3299 (m, br), 2222 (w), 1637 (s), 1598 (w), 1461 (s), 1440 (s), 1431 (s), 1387 (s), 1260 (m), 1196 (m), 1118 (s), 1087 (s), 952 (w), 815 (s), 777 (w), 758 (w), 738 (m), 676 (w), 651 (w), 619 (w) cm^{-1}. $C_{23}H_{25}ClMn_2N_{11}O_{11.5}$ (Dinuclear complex plus half a molecule of water) (784.84): calcd. C 35.20, H 3.21, N 19.63; found C 34.74, H 2.88, N 20.12.

$[Mn(bipy)_2(dcnm)_2]$ (9): (Me_4N)(dcnm) (50 mg, 297 μmol) in water (2 mL) was added to $Mn(ClO_4)_2{\cdot}6H_2O$ (25 mg, 69 μmol) in water (2 mL). 2,2′-Bipyridine (15 mg, 96 μmol) in methanol (1 mL) was added to this solution. Over four months crystals of the product formed from the solution, were washed with methanol and left to air-dry (18 mg, 67%). $C_{26}H_{16}MnN_{10}O_2$ (555.41): calcd. C 56.22, H 2.90, N 25.22; found C 56.34, H 3.01, N 25.43.

[Mn(bipy)$_2$(dcnm)(H$_2$O)](dcnm)·H$_2$O and (10) [Mn(bipy)$_2$(dcnm)-(H$_2$O)](dcnm) (11): (Me$_4$N)(dcnm) (50 mg, 297 μmol) in water (2 mL) was added to Mn(ClO$_4$)$_2$·6H$_2$O (25 mg, 69 μmol) in water (4 mL). 2,2′-Bipyridine (15 mg, 96 μmol) was then added as a solid and formed a white suspension. Overnight a crystal of **10** formed from the reaction solution for X-ray crystallography. Ten days later a crystal of **11** was removed from the reaction solution for X-ray crystallography. Both complexes co-crystallised from the reaction solution and their similar colour and morphology prohibited separation. The following day the bulk material was washed with methanol and ether and air-dried (4 mg, 15%). IR (ATR): $\tilde{\nu}$ = 3248 (vw), 3183 (vw), 3090 (vw), 2220 (m), 1621 (w), 1598 (m), 1576 (w), 1565 (w), 1473 (w), 1437 (s), 1384 (s), 1360 (s), 1316 (w), 1248 (vw), 1168 (s), 1153 (s), 1058 (w), 1014 (m), 758 (m), 735 (m) cm^{-1}. Elemental analysis indicates loss of intercalated water of **10** and partial loss of aqua ligands of **10** and **11** upon washing and atmospheric exposure. $C_{26}H_{17}MnN_{10}O_{2.5}$ (564.42): calcd. C 55.32, H 3.04, N 24.82; found C 55.20, H 3.12, N 25.02.

[Cu(cgnm)$_2$(H$_2$O)$_2$] (12): (Me$_4$N)(dcnm) (50 mg, 297 μmol) dissolved in ethylene glycol monomethyl ether (3 mL) was added to Cu(ClO$_4$)$_2$·6H$_2$O (53 mg, 143 μmol) in ethylene glycol monomethyl ether. After standing for two months the reaction solution was allowed to slowly evaporate over two months, yielding olive crystals of **12**, which were washed with ethanol and diethyl ether (42 mg, 66%). IR (ATR): $\tilde{\nu}$ = 3494 (m, br), 3254 (s, br), 2991 (w), 2945 (w), 2885 (m), 2219 (w), 1628 (s), 1470 (w), 1443 (m), 1412 (s), 1369 (m), 1307 (s), 1244 (w), 1161 (m), 1124 (s), 1098 (w/sh), 1031 (w), 1018 (w), 860 (w), 786 (w) cm^{-1}. $C_{12}H_{20}CuN_6O_8$ (439.87): calcd. C 32.77, H 4.58, N 19.11; found C 32.91, H 4.74, N 19.14.

Crystallographic Details and Data: Crystals were mounted on fine glass fibres using viscous hydrocarbon oil. Data were collected on a Bruker X8 Apex II CCD (**3**, **4**, **5**, **7**, **9**, **10**, **12**) or Nonius KappaCCD diffractometers (**1**, **2**, **6**, **8·3.4MeOH**, **11**), both equipped with graphite-monochromated Mo-K_α radiation (λ = 0.71073 Å). Data collection temperatures were maintained at 123 K using open flow N_2 cryostreams. For data collection with a Nonius KappaCCD diffractometer integration was carried out by the program DENZO-SMN and data were corrected for Lorentz-polarisation effects and for absorption using the program SCALEPACK.[44] Data integration for data collected with a Bruker X8 Apex II was carried out by the program SAINT and data was correct for Lorentz-polarization effects and for absorption using the Apex program II Suite.[45] Solutions were obtained by direct methods or Patterson synthesis using SHELXS-97[46] followed by successive refinements using full-matrix least-squares methods against F^2 using SHELXL-97.[46] The program X-Seed was used as a graphical SHELX interface.[47] Hydrogen atoms attached to carbon atoms were placed in idealised positions and refined against a riding model to the atom to which they are attached. Where possible, hydrogen atoms attached to nitrogen or oxygen atoms were located from the Fourier difference map (see individual crystal data).

CCDC-737442 (for **9**), -737443 (for **4**), -737444 (for **12**), -737445 (for **7**), -737446 (for **8**), -737447 (for **5**), -737448 (for **2**), -737449 (for **6**), -737450 (for **10**), -737451 (for **11**), -737452 (for **1**), -737453 (for **3**) contain the supplementary crystallographic data for this paper. These data can be obtained free of charge from The Cambridge Crystallographic Data Centre via www.ccdc.cam.ac.uk/data_request/cif.

[Cu$_3$(acnm)$_2$(dmae)$_2$(H$_2$O)$_2$] (1): $C_{14}H_{26}Cu_3N_8O_8$, M = 625.05, blue plate, 0.30 × 0.30 × 0.10 mm^3, triclinic, space group $P\bar{1}$ (No. 2), a = 7.2289(3), b = 7.5089(3), c = 10.7812(5) Å, α = 87.667(2), β = 80.702(2), γ = 88.411(3)°, V = 576.91(4) Å^3, Z = 1, D_c = 1.799 g/cm^3, F(000) = 317, $2\theta_{max}$ = 55.0°, 2926 reflections collected, 2287 unique (R_{int} = 0.1010). Final $GooF$ = 1.022, R_1 = 0.0647, wR_2 = 0.1645, R indices based on 1687 reflections with $I > 2\sigma(I)$ (refinement on F^2), 165 parameters, 3 restraints. μ = 2.797 mm^{-1}. Hydrogen atoms attached to nitrogen and oxygen atoms were located from the Fourier difference map and restrained with the DFIX command.

[Cu(acnm)(NH$_3$)$_2$]$_\infty$ (2): $C_3H_7CuN_5O_2$, M = 208.68, blue block, 0.30 × 0.20 × 0.20 mm^3, monoclinic, space group $P2_1/n$ (No. 14), a = 8.0740(2), b = 6.6300(2), c = 12.7203(4) Å, β = 103.294(1)°, V = 662.7(2) Å^3, Z = 4, D_c = 2.092 g/cm^3, F(000) = 420, $2\theta_{max}$ = 55.0°, 3874 reflections collected, 1526 unique (R_{int} = 0.0538). Final $GooF$ = 1.048, R_1 = 0.0307, wR_2 = 0.0753, R indices based on 1343 reflections with $I > 2\sigma(I)$ (refinement on F^2), 128 parameters, 7 restraints. μ = 3.249 mm^{-1}. Hydrogen atoms attached to nitrogen atoms were located from the Fourier difference map and restrained with the DFIX command.

[Cu(acnm)(NH$_3$)$_2$(py)] (3): $C_8H_{12}CuN_6O_2$, M = 287.78, blue block, 0.20 × 0.20 × 0.15 mm^3, orthorhombic, space group $Pbca$ (No. 61), a = 13.1902(3), b = 13.2981(3), c = 13.4531(3) Å, V = 2359.74(9) Å^3, Z = 8, D_c = 1.620 g/cm^3, F(000) = 1176, $2\theta_{max}$ = 55.0°, 13107 reflections collected, 2696 unique (R_{int} = 0.0214). Final $GooF$ = 1.066, R_1 = 0.0201, wR_2 = 0.0525, R indices based on 2451 reflections with $I > 2\sigma(I)$ (refinement on F^2), 182 parameters, 7 restraints. μ = 1.852 mm^{-1}. Hydrogen atoms attached to nitrogen atoms were located from the Fourier difference map and restrained with the DFIX command.

[Cu(cenm)$_2$(H$_2$O)$_2$] (4): $C_{10}H_{16}CuN_6O_6$, M = 379.83, green needle, 0.20 × 0.10 × 0.04 mm^3, triclinic, space group $P\bar{1}$ (No. 2), a = 5.0402(4), b = 6.8373(5), c = 11.8858(8) Å, α = 75.828(4), β = 85.379(4), γ = 81.262(4)°, V = 392.12(5) Å^3, Z = 1, D_c = 1.608 g/cm^3, F(000) = 195, T = 200(1) K, $2\theta_{max}$ = 55.0°, 4125 reflections collected, 1801 unique (R_{int} = 0.0201). Final $GooF$ = 1.099, R_1 = 0.0277, wR_2 = 0.0613, R indices based on 1742 reflections with $I > 2\sigma(I)$ (refinement on F^2), 119 parameters, 0 restraints. μ = 1.433 mm^{-1}.

{[Cu(cenm)$_2$]$_2$·H$_2$O}$_\infty$ (5): $C_{20}H_{26}Cu_2N_{12}O_9$, M = 705.61, Green block, 0.25 × 0.23 × 0.20 mm^3, monoclinic, space group $C2/c$ (No. 15), a = 16.0822(3), b = 17.8062(4), c = 12.1685(2) Å, β = 123.9700(10)°, V = 2889.89(10) Å^3, Z = 4, D_c = 1.622 g/cm^3, F(000) = 1440, $2\theta_{max}$ = 55.0°, 9860 reflections collected, 3281 unique (R_{int} = 0.0231). Final $GooF$ = 1.056, R_1 = 0.0264, wR_2 = 0.0622, R indices based on 2933 reflections with $I > 2\sigma(I)$ (refinement on F^2), 209 parameters, 1 restraint. Lp and absorption corrections applied, μ = 1.541 mm^{-1}. Hydrogen atoms attached to nitrogen and oxygen atoms were located from the Fourier difference map and restrained with the DFIX command.

{[Mn$_3$(ccnm)$_2$(EtOH)$_2$(OAc)$_4$]·2EtOH}$_\infty$ (6): $C_{22}H_{40}Mn_3N_6O_{16}$, M = 809.42, orange diamond, 0.20 × 0.20 × 0.10 mm^3, triclinic, space group $P\bar{1}$ (No. 2), a = 9.0675(18), b = 9.5203(19), c = 11.012(2) Å, α = 103.961(4), β = 101.049(5), γ = 98.456(6)°, V = 886.6(3) Å^3, Z = 1, D_c = 1.516 g/cm^3, F(000) = 417, $2\theta_{max}$ = 55.0°, 8738 reflections collected, 4032 unique (R_{int} = 0.1131). Final $GooF$ = 1.018, R_1 = 0.0564, wR_2 = 0.1272, R indices based on 2906 reflections with $I > 2\sigma(I)$ (refinement on F^2), 226 parameters, 2 restraints. μ = 1.125 mm^{-1}. Hydrogen atoms attached to oxygen atoms were located from the Fourier difference map and restrained with the DFIX command.

(Et$_4$N)$_2$[Cu(ccnm)$_4$] (7): $C_{28}H_{48}CuN_{14}O_8$, M = 772.34, green needle, 0.50 × 0.30 × 0.15 mm^3, monoclinic, space group $P2_1/n$ (No. 14), a = 10.3502(3), b = 10.1528(3), c = 16.9498(5) Å, β = 93.916(2)°, V

= 1776.99(9) Å^3, Z = 2, D_c = 1.443 g/cm^3, F(000) = 814, $2\theta_{max}$ = 55.0°, 14294 reflections collected, 4077 unique (R_{int} = 0.0289). Final *GooF* = 1.049, R_1 = 0.0512, wR_2 = 0.1297, R indices based on 3466 reflections with $I>2\sigma(I)$ (refinement on F^2), 236 parameters, 0 restraints. μ = 0.683 mm^{-1}. Hydrogen atoms attached to nitrogen atoms were located from the Fourier difference map and restrained with the DFIX command.

[Mn(cmnm)$_3$Mn(bipy)(MeOH)](ClO$_4$)·3.4MeOH (8·3.4MeOH): $C_{26.40}H_{37.60}ClMn_2N_{11}O_{14.40}$, M = 884.80, red block, 0.20×0.20×0.10 mm^3, monoclinic, space group $P2_1/m$ (No. 11), a = 8.8914(2), b = 13.386(4), c = 16.349(5) Å, β = 102.49(1)°, V = 1899.9(7) Å^3, Z = 2, D_c = 1.547 g/cm^3, F(000) = 910, $2\theta_{max}$ = 55.0°, 12001 reflections collected, 4556 unique (R_{int} = 0.1173). Final *GooF* = 0.974, R_1 = 0.0581, wR_2 = 0.1251, R indices based on 2519 reflections with $I>2\sigma(I)$ (refinement on F^2), 318 parameters, 10 restraints. μ = 0.814 mm^{-1}. Hydrogen atoms attached to nitrogen atoms were located from the Fourier difference map and allowed to refine freely. The alcohol hydrogen atoms of the methanol molecules could not be located in Fourier difference map and were not refined. Carbon to oxygen bond lengths in the disordered methanol molecules were restrained with the DFIX command. The asymmetric unit contains one methanol disordered over two positions with site occupancies refined against each other (37:63). A further partial occupancy methanol (70%) was manually refined in two positions (20:50).

[Mn(bipy)$_2$(dcnm)$_2$] (9): $C_{26}H_{16}Mn_1N_{10}O_2$, M = 555.43, orange prism, 0.22×0.18×0.15 mm^3, triclinic, space group $P\bar{1}$ (No. 2), a = 9.0435(2), b = 10.3753(2), c = 15.1752(3) Å, α = 79.610(1), β = 87.609(1), γ = 65.608(1)°, V = 1274.67(5) Å^3, Z = 2, D_c = 1.447 g/cm^3, F(000) = 566, $2\theta_{max}$ = 55.0°, 10585 reflections collected, 5854 unique (R_{int} = 0.0212). Final *GooF* = 1.028, R_1 = 0.0331, wR_2 = 0.0764, R indices based on 5187 reflections with $I>2\sigma(I)$ (refinement on F^2), 352 parameters, 0 restraints μ = 0.563 mm^{-1}.

[Mn(bipy)$_2$(dcnm)(H$_2$O)](dcnm)·H$_2$O (10): $C_{26}H_{20}MnN_{10}O_4$, M = 591.46, orange block, 0.60×0.50×0.30 mm^3, triclinic, space group $P\bar{1}$ (No. 2), a = 9.5202(3), b = 11.8669(4), c = 13.3734(4) Å, α = 65.043(1), β = 89.887(1), γ = 79.199(1)°, V = 1340.47(7) Å^3, Z = 2, D_c = 1.465 g/cm^3, F(000) = 602, $2\theta_{max}$ = 55.0°, 9286 reflections collected, 5841 unique (R_{int} = 0.0170). Final *GooF* = 1.038, R_1 = 0.0457, wR_2 = 0.1235, R indices based on 5338 reflections with $I>2\sigma(I)$ (refinement on F^2), 415 parameters, 12 restraints. μ = 0.546 mm^{-1}. Free dcnm bond lengths restrained by DFIX, and the anion was disordered over two positions. Site occupancies were refined against each other (54:46) although ADP values indicate further disorder. Hydrogen atoms attached to the free water molecule could not be located from the Fourier transform map and were not refined. Hydrogen atoms attached to coordinating water molecule were located from the Fourier difference map and restrained with the DFIX command.

[Mn(bipy)$_2$(dcnm)(H$_2$O)](dcnm) (11): $C_{26}H_{18}MnN_{10}O_3$, M = 573.44, orange block, 0.60×0.40×0.30 mm^3, monoclinic, space group $P2_1/c$ (No. 14), a = 11.0537(2), b = 16.9890(3), c = 14.8872(3) Å, β = 110.210(10)°, V = 2623.56(8) Å^3, Z = 4, D_c = 1.452 g/cm^3, F(000) = 1172, $2\theta_{max}$ = 55.0°, 12937 reflections collected, 6034 unique (R_{int} = 0.0847). Final *GooF* = 1.061, R_1 = 0.0458, wR_2 = 0.1062, R indices based on 4734 reflections with $I>2\sigma(I)$ (refinement on F^2), 388 parameters, 6 restraints. μ = 0.552 mm^{-1}. Free dcnm bond lengths were restrained by DFIX, and the nitroso groups were disordered over two positions with site occupancies refined against each other (56:44) although ADP values indicate further disorder. Disordered nitrile groups could not be accurately refined separately. Hydrogen atoms attached to the coordinating water molecule were located from the Fourier difference map and restrained with the DFIX command.

[Cu(cgnm)$_2$(H$_2$O)$_2$] (12): $C_{12}H_{20}CuN_6O_8$, M = 439.88, green plate, 0.30×0.30×0.10 mm^3, triclinic, space group $P\bar{1}$ (No. 2), a = 4.8634(2), b = 6.9532(2), c = 13.9302(5) Å, α = 79.564(2), β = 87.168(2), γ = 80.869(2)°, V = 457.30(3) Å^3, Z = 1, D_c = 1.597 g/cm^3, F(000) = 227, $2\theta_{max}$ = 55.0°, 4810 reflections collected, 2090 unique (R_{int} = 0.0233). Final *GooF* = 1.041, R_1 = 0.0271, wR_2 = 0.0651, R indices based on 2008 reflections with $I>2\sigma(I)$ (refinement on F^2), 137 parameters, 3 restraints. μ = 1.248 mm^{-1}.

Magnetic Susceptibility Measurements: Powder samples of mass ca. 20 mg were accurately weighed and contained in calibrated gel capsules that were held rigidly in the centre of a drinking straw that was fixed to the end of the sample rod, the latter being inserted into the sample chamber of a Quantum Design liquid helium MPMS5 Squid magnetometer. The applied DC field used was 1 Tesla and the instrument was calibrated against the accurately known magnetisation values of a Pd pellet, supplied by Quantum Design, and further checked against the well known Curie–Weiss molar susceptibility data of $CuSO_4·5H_2O$. Diamagnetic corrections for the ligands were obtained using Pascal's tables.

Acknowledgments

We thank the Australian Research Council for funding to S. R. B. and K. S. M. and for a postdoctoral fellowship (to D. R. T.). A. S. R. C. acknowledges the award of an Australian Postgraduate Award scholarship.

[1] J. Kohout, M. Hvastijová, J. Gažo, *Coord. Chem. Rev.* **1978**, *27*, 141–172.
[2] a) J. Kožíšek, M. Hvastijová, J. Kohout, *Inorg. Chim. Acta* **1990**, *168*, 157–158; b) M.-L. Tong, Y.-M. Wu, Y.-X. Tong, X.-M. Chen, H.-C. Chang, S. Kitagawa, *Eur. J. Inorg. Chem.* **2003**, 2385–2388.
[3] M. Hvastijová, J. Kohout, H. Köhler, G. Ondrejovič, *Z. Anorg. Allg. Chem.* **1988**, *566*, 111–120.
[4] M. Hvastijová, J. Kohout, R. Skirl, *Collect. Czech. Chem. Commun.* **1993**, *58*, 845.
[5] J. K. Bjernemose, C. J. McKenzie, P. R. Raithby, S. J. Teat, *Dalton Trans.* **2003**, 2639–2640.
[6] M. Hvastijová, J. Kohout, J. W. Buchler, R. Boča, J. Kožíšek, L. Jäger, *Coord. Chem. Rev.* **1998**, *175*, 17–42.
[7] A. S. R. Chesman, D. R. Turner, G. B. Deacon, S. R. Batten, *Chem. Asian J.* **2009**, *4*, 761–769.
[8] N. Arulsamy, D. Bohle, *J. Org. Chem.* **2000**, *65*, 1139–1143.
[9] Y. M. Chow, D. Britton, *Acta Crystallogr., Sect. B* **1974**, *30*, 1117–1118.
[10] a) N. Arulsamy, D. S. Bohle, B. G. Doletski, *Inorg. Chem.* **1999**, *38*, 2709–2715; b) G. Glover, N. Gerasimchuk, R. Biagioni, K. V. Domasevitch, *Inorg. Chem.* **2009**, *48*, 2371–2382.
[11] Y. M. Chow, D. Britton, *Acta Crystallogr., Sect. B* **1974**, *30*, 147–151.
[12] D. J. Price, S. R. Batten, K. J. Berry, B. Moubaraki, K. S. Murray, *Polyhedron* **2003**, *22*, 165–176.
[13] V. Jacob, S. Mann, G. Huttner, O. Walter, L. Zsolnai, E. Kaifer, P. Rutsch, P. Kircher, E. Bill, *Eur. J. Inorg. Chem.* **2001**, *10*, 2625–2640.
[14] N. N. Gerasimchuk, N. K. Dalley, *J. Coord. Chem.* **2004**, *57*, 1431–1445.
[15] K. E. Bessler, L. L. Romualdo, P. d. T. S. Filho, V. M. Deflon, C. Maichle-Mössmer, *Z. Anorg. Allg. Chem.* **2001**, *627*, 651–654.
[16] D. R. Turner, S. R. Batten, *Coordination Chemistry Research Progress* (Eds.: T. W. Cartere, K. S. Verley), Nova Science Publishers, Hauppauge, **2008**.

[17] A. S. R. Chesman, D. R. Turner, B. Moubaraki, K. S. Murray, G. B. Deacon, S. R. Batten, *Chem. Eur. J.* **2009**, *15*, 5203–5207.
[18] D. R. Turner, S. N. Pek, S. R. Batten, *Chem. Asian J.* **2007**, *2*, 1534–1539.
[19] D. R. Turner, S. R. Batten, *CrystEngComm* **2008**, *10*, 170–172.
[20] D. R. Turner, S. N. Pek, S. R. Batten, *New J. Chem.* **2008**, *32*, 719–726.
[21] D. R. Turner, S. N. Pek, S. R. Batten, *CrystEngCommun* **2009**, *11*, 87–93.
[22] D. R. Turner, R. MacDonald, W. T. Lee, S. R. Batten, *CrystEngComm* **2009**, *11*, 298–305.
[23] D. R. Turner, S. N. Pek, J. D. Cashion, B. Moubaraki, K. S. Murray, S. R. Batten, *Dalton Trans.* **2008**, 6877–6879.
[24] S. R. Batten, K. S. Murray, *Coord. Chem. Rev.* **2003**, *246*, 103–130.
[25] A. S. R. Chesman, D. R. Turner, D. J. Price, B. Moubaraki, K. S. Murray, G. B. Deacon, S. R. Batten, *Chem. Commun.* **2007**, 3541–3543.
[26] a) N. Gerasimchuk, L. Goeden, P. Durham, C. Barnes, J. F. Cannon, S. Silchenko, I. Hidalgo, *Inorg. Chim. Acta* **2008**, *361*, 1983–2001; b) N. Gerasimchuk, T. Maher, P. Durham, K. V. Domasevitch, J. Wilking, A. Mokhir, *Inorg. Chem.* **2007**, *46*, 7268–7284; c) D. Eddings, C. Barnes, N. Gerasimchuk, P. Durham, K. Domasevich, *Inorg. Chem.* **2004**, *43*, 3894–3909.
[27] a) T. Y. Sliva, A. M. Duda, T. Glowiak, I. O. Fritsky, V. M. Amirkhanov, A. A. Mokhir, H. Kozlowski, *J. Chem. Soc., Dalton Trans.* **1997**, 273–276; b) A. A. Mokhir, R. Vilaplana, F. Gonzalez-Vilchez, I. O. Fritsky, K. V. Domasevitch, N. M. Dudarenko, *Polyhedron* **1998**, *17*, 2693–2697.
[28] M. Hvastijová, J. Kohout, J. Kožíšek, L. Jäger, I. Svoboda, Monograph Series of the International Conferences on Coordination Chemistry held periodically at Smolenice in Slovakia, **1997**, *3*, 159–164, Slovak Technical University Press.
[29] Z. Xu, L. K. Thompson, D. O. Miller, *Chem. Commun.* **2001**, 1170–1171.
[30] I. Potočňák, M. Vavra, L. Jäger, P. Baran, C. Wagner, *Transition Met. Chem.* **2008**, *33*, 1–8.
[31] M. Dunaj-Jurčo, D. Mikloš, I. Potočňák, L. Jäger, *Acta Crystallogr., Sect. C* **1998**, *54*, 1763–1765.
[32] W. Mazurek, K. J. Berry, K. S. Murray, M. J. O' Connor, M. R. Snow, A. G. Wedd, *Inorg. Chem.* **1982**, *21*, 3071–3080.
[33] F. Birkelbach, M. Winter, U. Flörke, H.-J. Haupt, C. Butzlaff, M. Lengen, E. Bill, A. X. Trautwein, K. Wieghardt, P. Chaudhuri, *Inorg. Chem.* **1994**, *33*, 3990–4001.
[34] R. Veit, J. J. Girerd, O. Kahn, F. Roberts, Y. Jeannin, *Inorg. Chem.* **1986**, *25*, 4175–4180.
[35] P. Chaudhuri, M. Winter, B. P. C. Della Védova, E. Bill, A. Trautwein, S. Gehring, P. Fleischauer, B. Nuber, J. Weiss, *Inorg. Chem.* **1991**, *30*, 2148–2157.
[36] B. Bleaney, K. D. Bowers, *Proc. R. Soc. London, Sect. A* **1952**, *214*, 451–465.
[37] D. S. Bohle, B. J. Conklin, C.-H. Hung, *Inorg. Chem.* **1995**, *34*, 2569–2581.
[38] R. Boča, M. Hvastijová, J. Kožíšek, *J. Chem. Soc., Dalton Trans.* **1995**, 1921–1923.
[39] S. Ross, T. Weyermüller, E. Bill, K. Wieghardt, P. Chaudhuri, *Inorg. Chem.* **2001**, *40*, 6656–6665.
[40] P. Chaudhuri, *Coord. Chem. Rev.* **2003**, *243*, 143–190.
[41] C. J. Milios, W. Wernsdorfer, S. Moggach, S. Parsons, S. P. Perlepes, G. Christou, E. K. Brechin, *J. Am. Chem. Soc.* **2007**, *129*, 2754–2755.
[42] H.-B. Zu, B.-W. Wang, F. Pan, Z.-M. Wang, S. Gao, *Angew. Chem. Int. Ed.* **2007**, *46*, 7388–7392.
[43] G. Longo, *Gazz. Chim. Ital.* **1931**, *61*, 575.
[44] Z. Otwinowski, W. Minor (Eds.), *Methods in* Enzymology, vol. 276 (Eds.: C. W. Carter Jr., R. M. Sweet), p. 99, 307–326, Academic Press, New York, **1997**.
[45] *ApexII*, v2.1.0, Bruker AXS Ltd., Madison, Wisconsin, **2005**.
[46] G. M. Sheldrick, *Acta Crystallogr., Sect. A* **2008**, *64*, 112–122.
[47] L. J. Barbour, *J. Supramol. Chem.* **2001**, *1*, 189–191.

Received: August 10, 2009
Published Online: November 26, 2009

